C.P. No. 908

MINISTRY OF AVIATION

AERONAUTICAL RESEARCH COUNCIL

CURRENT PAPERS

Gun Tunnel Measurements of Lift, Drag and pitching Moment on a 20° Cone, a Flat Delta and a Caret Delta Wing at a Mach number of 8.3

By

T. Opatowski
Imperial College of Science and Technology

LONDON: HER MAJESTY'S STATIONERY OFFICE

1966

Price 10s. 6d. net

C.P. No.908

December, 1965

Gun Tunnel Measurements of Lift, Drag and Pitching Moment on a 20° Cone, a Flat Delta and a Caret Delta Wing at a Mach number of 8·3

- By -
T. Opatowski,
Imperial College of Science and Technology

Communicated by Prof. P. R. Owen

SUMMARY

Measurements of lift drag and pitching moment have been made on a 20° half-angle, right-circular cone and on two delta wings of triangular and caret cross section, 10° wedge angle and aspect ratio 1 in the Imperial College gun tunnel.

The strain gauge balance developed for this purpose gave results which were within 5% of other published cone data.

Maximum lift/drag ratios of about 3·7 were obtained for both wings at the test Mach number of 8·3 and Reynolds number based on root chord of $1{\cdot}5 \times 10^6$.

The measured lift, drag and lift/drag ratio agreed well with estimates based on two-dimensional oblique shock theory and laminar skin friction.

List/

Replaces A.R.C. 27 582

List of Contents

---

1. Introduction

The object of the work, which is covered in part by this report, was to make force measurements in the gun tunnel on models of hypersonic lifting vehicles. This entailed considerable modification and development of an existing strain gauge balance. Other strain gauge balances for short duration facilities have either been inertia compensated (e.g., Ref. 14) or made extremely stiff with electronic filtering of the vibratory signal components (e.g., Ref. 12). As the natural frequency of the present balance plus models was too low for electronic filtering a hydraulic damper was fitted.

A 20° half-angle cone was chosen as a calibration model and showed, by comparison with existing data from conventional wind tunnels, that reasonable results could be obtained. The two delta wings tested, one plain and one caret or Nonweiler, were the first of a series of slender wings to be tested and though they presented a more difficult task for the balance, useful results have also been obtained.

2. The Gun Tunnel Balance

2.1 Physical details

The layout of the modified balance is shown in Fig. 1(a) and diagramatically in Fig. 1(b). There are three cantilevers (A, B & C) in what was part of the original balance and these are connected through the flexure hinges (D) to the balance beam via tapered pins. The aft cantilever measures drag while the other two together measure lift and were intended to measure pitching moment, but proved insufficiently accurate for this purpose.

At the front of the balance beam is mounted a combined moment sensor and incidence adjustor. The whole unit (E & F) is free to rotate about a phosphor bronze bush (J) but the end of the moment sub-beam (E) is restrained by a pin which is free to slide fore and aft in the balance beam.

The catch shown (G) together with another underneath, not shown, connect the model mounting plate to the moment sub-beam allowing incidence adjustments in steps of $7\frac{1}{2}°$. Adjustment within these steps was accomplished by tilting the whole balance on a special mount.

Damping was provided by the hydraulic damper (H). Highly viscous silicon fluid of 10^5 centistoke was used and the desired damping achieved by progressively reducing the size of the piston. In the optimum damping configuration the piston was less than half the area of the dashpot. Typical lift traces with and without damping are given in Fig. 2(b).

The lift and drag cantilevers used foil type Budd gauges while the moment sensor used two silicon strain gauges (Type 3A-1A-120P made by Ether Ltd.). These gauges have a sensitivity sixty times that of the foil gauges. Silicon gauges change their resistance and gauge factor with temperature, a characteristic that causes difficulties in continuous facilities necessitating special compensating techniques (see Ref. 15 for example). No change in temperature occurred during the short running time of the gun tunnel (checked by recording the output of the bridge in the 'calibrate' configuration (Fig. 3) and hence its resistance through a run) and it was

found/

found possible to allow for variations caused by atmospheric changes of temperature by measuring the gauge resistance before each run. The P type gauges have the larger variation of resistance with temperature and these were chosen to give the best sensitivity in determining the temperature and hence gauge factor (see Fig. A1).

The circuit for the moment sensor is shown in Fig. 3. All channels were fed from a 9v stabilized voltage source but the voltage input to the moment channel was dropped to 3v by resistors. The six component bridge network in the moment channel (Fig. 3) was so arranged that for test each gauge was in a separate leg of a Wheatstone bridge circuit while for gauge factor measurement both gauges were in one leg of the bridge. The arrangement of the voltage dropping resistors was such that the current through the gauges was approximately the same when switched to 'test' or 'calibrate' in order to maintain a constant level of self-heating.

2.2 Performance

Because of mishandling the balance was slightly strained and this resulted in non-linear readings which changed slightly from time to time. It was essential to check the calibration frequently in order to achieve reliable data. Calibrations were carried out before and after each series of tests with spot checks about every ten runs as shown in Figures A1 to A5.

The load capacity of the balance was:-

Lift	10 lb
Drag	24 lb
Moment	200 lb in.

and the sensitivities were approximately

Lift, front	0·54 mv/lb
Lift, rear	0·33 mv/lb
Drag	0·16 mv/lb
Moment	1·82 mv/lb in.

The vibratory frequencies were complicated by the damper which tended to couple the lift and drag. With the cone model which weighed 51 gm a predominant 170 c.p.s. was evident on the lift trace (shown in Fig. 2(a)) and this seemed to be superimposed on an aperiodic decay. The level of damping was chosen to ensure that the mean line had reached its steady value; which limited the amount of damping possible on the higher frequency mode.

The wing models, which weighed 135 gm were mounted much further forward on the balance and had a dominant lift frequency (damped) of 100 c.p.s. The drag traces were very irregular with no clearly dominant frequency. Typical drag traces are given in Fig. 2.

As/

As the model centres of gravity were not at the moment pivot point (para. 2.1) the lift vibrations were reflected in the moment trace. The natural frequency of the moment cantilever was calculated to be 500 c.p.s. and was not discernible on the traces.

The main unusual design features, namely the use of uncompensated silicon gauges, the plain bearing and the hydraulic damper; worked satisfactorily. The change in gauge factor due to temperature change was never more than 3% during these tests and could be determined to better than 5% of this 3% variation. The friction from the plain bearing made calibration more difficult but gave no trouble in use because of the short running time during which the readings never settled completely. By calibrating with increasing and decreasing loads and with extreme care, consistent calibrations were achieved.

Full details of the balance calibration are given in Appendix A.

3. Force Measurements

3.1 Models tested

The cone and delta wing models are shown in Fig. 4, together with their relevant physical details. A $2\frac{1}{2}$ in. diameter hemisphere was also tested for tunnel calibration purposes. (See para. 4.1).

The angle between the plane of the leading edge and the lower ridge line of the caret wing was 6°. At the test Mach number of 8·3 this would result in the shock lying in the leading edge plane at 4° and 16° incidence for inviscid 2-D flow and be within 0·7° of this plane between the above angles[7].

3.2 Test conditions

The cone was tested at incidences up to 30° in steps of $7\frac{1}{2}$°. The moment pivot was located at about the 3/4 chord point of the cone and this limited the incidence obtainable to 37° as the base of the cone came in contact with the balance beam.

The wings were tested in the incidence range α = 5° to 16°, the upper limit being dictated by balance strength considerations.

The actual incidences in the case of the cone were determined with a precision protractor. The deflection under load was negligible (see Appendix A). In the case of the wings two methods were used. The flat bottomed wing was measured with an inclinometer of known weight and the deflection under load measured and allowed for. The incidence was also measured from the schlieren photographs. The two methods agreed to within a maximum difference of 0·2°.

The tests were performed in the Imperial College gun tunnel described in Ref. 1. Since that report, the conical nozzle has been replaced by a Mach 8 (nominal) contoured nozzle. With atmospheric pressure in the barrel the test conditions were:-

Driving Pressure p.s.i.	Mach No.	Re/Inch
2000	8·25	$0·23 \times 10^6$
1000	8·3	$0·17 \times 10^6$

The/

The calibration of the contoured nozzle was carried out at 2000 p.s.i. driving pressure and gave a mean Mach number of 8·25 with negligible Mach number gradient. The test Mach number at 1000 p.s.i. driving pressure was deduced from drag measurements on a hemisphere as described in para. 4.1. Most of the tests were carried out at 1000 p.s.i. driver pressure because of balance strength limitations.

All the wing tests were run with 1000 p.s.i. driver pressure and 40 p.s.i.a. in the barrel giving a Reynolds number per inch of $0{\cdot}296 \times 10^6$ in the free stream.

4. Results and Discussion

4.1 Hemisphere

The drag coefficient of the hemisphere measured with 2000 p.s.i. driving pressure at a Mach number of 8·25 was 0·915. This compared well with that given, for example, by Hoerner[2] and served as a check on both the balance and the tunnel calibration. The hemisphere was then used to determine the effective Mach number when operating with 1000 p.s.i. driving pressure, using the calibration of the reservoir pressure of the tunnel given in Ref. 1.

4.2 20° Cone

Figures 5, 6 and 7 give the measured lift coefficient, drag coefficient and centre of pressure position against incidence, respectively.

Also plotted on these figures are some experimental results from several sources[3,4,5,6], and Newtonian values as calculated in Ref. 3. In each case the coefficients are based on plan area.

Good agreement with both experiment and Newtonian theory has been achieved in each case. The lift coefficient would appear to be somewhat higher than the comparative results but the difference is within the accuracy of the balance (see para. 5.3). The conditions of the comparative tests ranged from $M_N = 6{\cdot}8$ to $M_N = 9{\cdot}6$ and $Re = 0{\cdot}56 \times 10^6$ to $1{\cdot}2 \times 10^6$ thus bridging the conditions of the present experiments.

The drag and pitching moments are in excellent agreement. The pitching moment was so close to zero that it has had to be plotted on a very much expanded scale.

4.3 Delta wings

4.3.1 Lift

The measured values are compared with two simple theoretical estimates in Figure 8. For the full line in the figure, two-dimensional flow has been assumed to exist on all surfaces (i.e., as if the surface was part of an infinite unswept plane) and the appropriate oblique shock or expansion pressures from Ref. 7 used to determine the lift coefficient. The under surface of the caret wing has been assumed to have two-dimensional flow over it for all the incidences tested and hence the two wings have the same estimated pressures on this surface. Thus the estimated lifts cannot show any direct benefit from the caret configuration. Allowance has also been made for the effect of boundary-layer thickness (see para. 4.3.2) though this only amounted to about 0·002 in lift coefficient.

The/

The dashed line is the Newtonian value using $C_p = 2 \sin^2\delta$ and the appropriate flow deflection angles (δ) for all surfaces.

Good agreement with the two-dimensional approximation has been obtained.

This is in accord with the recent numerical solutions of Babaev[16]. Although his solutions do not cover the present configuration, a mean pressure on the under surface of the order of 3 - 4% less than the true 2-D value would be indicated by his results and it is possible to see a difference of this order between the plain and caret wing results at the higher incidences where the influence of the upper surfaces is least.

Babaev's solutions apply strictly only to flows with attached leading edge shocks. For the plain delta of the present tests, shock detachment would be expected to occur at about 7° incidence. This is substantiated by the plan view schlieren photographs presented in Figs. 12 (d)-(g) and discussed in para. 4.3.4. The fact that the difference between the plain and caret wings was still of the order of magnitude indicated by Babaev's work suggests that slight shock detachment has only a small effect on the results for truly independent surfaces. This can also be deduced from Squire's results[19] where pressures close to those obtained from oblique attached shock theory were measured on the lower surface of a flat delta wing despite shock detachment due to the incidence of the upper surface.

The Newtonian estimate of lift is poor, as might be expected at these low flow deflection angles and moderate Mach numbers.

4.3.2 Drag

The experimental and theoretical drag results are shown in Fig. 9. The inviscid part of the theoretical drag was obtained in the same way as the theoretical lift.

Laminar flow has been assumed throughout and this was largely confirmed by schlieren photographs though in a few cases the flow appeared transitional towards the trailing edge of the root chord. The skin friction drag and boundary-layer thickness were calculated using the methods given by Monaghan[8], and Catherall[9], assuming that each streamwise strip was independent of its neighbour and behaved as a sharp flat plate with zero pressure gradient with appropriate free stream conditions. The free stream conditions used were those calculated for the inviscid lift (see para. 4.3.1).

The base pressure has been taken as half the free stream static pressure which is approximately the value given by King[10], for conditions similar to these tests. This value was also found in measurements made by McLellan, Bertram and Moore[13], on the base of a 20° wedge at a Mach number of 6·9 and Reynolds number of $0{\cdot}98 \times 10^6$.

The agreement of the experimental results with the theoretical drags obtained as above is reasonably good. The measured drags were generally slightly higher than the theoretical for both wings but both values are amply covered by the possible inaccuracies of the balance. The effect of leading edge sweep, three-dimensionality of the flow and the streamwise corner on the caret wing on the boundary layer or on transition have not been considered.

The/

The boundary-layer corrections to drag and lift have been included for each surface by taking the trailing edge, centre line displacement thickness (δ^*root) calculated as stated before and assuming an effective change of surface incidence given by $\frac{\delta^* \text{ root}}{\ell}$, where ℓ is the model length.

Leading edge boundary-layer interaction would not be expected to have any significant effect under the test conditions[11].

As would be expected, both the theory and measured results show the caret wing to have a higher drag at incidence due to its greater wetted area. At lower incidences this is offset to some extent by the greater anhedral of the upper surface which gives less lift reduction. The greater drag is also offset in practice, though not in the present theory, by the slightly higher lift developed by the caret wing.

Newtonian theory, even with skin friction added, can again be seen to give a poor estimate.

4.3.3 Lift drag ratio

The measured and theoretical lift/drag ratios are shown in Fig. 10. Fortuitously, the Newtonian theory with laminar skin friction added now shows excellent agreement with the experimental data.

A maximum lift/drag ratio of about 3·7 was obtained in both cases. All the differences between the maximum lift/drag ratios, both measured and theoretical, are small and it is evident that the extra drag of the caret wing is balanced by the decreased lift of the plain delta.

The results agree well with similar measurements obtained by Becker[17], and Blackstock and Ladson[18].

4.3.4 Shock angles

The centre line shock angles were measured from schlieren photographs, and are plotted in Fig. 12(a). These angles corrected for boundary-layer displacement are also plotted and hence the size of the correction can be seen. Also plotted are the two-dimensional and conical shock angles. The shock angles on the caret wing were close to the two-dimensional values while the plain delta shock angles lay between the two-dimensional and the conical values as given in Ref. 7.

Typical schlieren photographs in side and plan view are presented in Figs. 12(b)-(g). The side view photographs are for incidences of approximately 10°, the 'design' incidence, when the upper surfaces of both models are streamwise.

The plan view photographs show the plain delta wing at 6°, 10° and 16° incidence and the caret delta at 16° incidence. At 6° the shock is still attached to the leading edge of the plain delta while it is slightly detached at 10°. At 16° the detachment is more noticeable while, by contrast, the shock is still attached on the caret wing for which this is the upper design shock closure angle.

4.3.5/

4.3.5 Centre of pressure position

Fig. 11 gives the measured centre of pressure positions. These models were the thinnest that could be accommodated on the balance and had to be mounted well forward of the moment sensor. This resulted in poor accuracy as compared to the cone results where the sensor could be buried in the model. (See para. 5.6.) All that can be said is that the C.P. was at about the expected 2/3 chord position.

5. Accuracy of Results

5.1 General

For those traces which exhibited a sinusoidal and decaying wave form the mean line could be determined quite accurately. The measurements were taken to 0·2 millimetres but were probably not repeatable to better than 0·7 millimetre.

Assuming a typical trace deflection of $3\frac{1}{2}$ cm for lift and moment this gives ± 2% reading accuracy.

A better estimate of the performance than the worst possible error is probably that error which is exceeded on say less than 20% of occasions and it is with this concept in mind that the following accuracies have been assessed, in so far as the greater errors of occasional traces with poor wave forms have been ignored.

5.2 Moments

The moment sensor was independent of the other channels and the obtainable accuracy is assessed at ± 3%, being made up from a calibration error of ± 1% and an error in trace reading of ± 2%.

5.3 Lift

In order to get a realistic estimate of the accuracy of the balance, the maximum possible errors for a typical run (wing), corresponding to a mean lift coefficient of 0·15, have been calculated with the following results:

Trace reading ± 2% of lift reading

Calibration ± 3% " " "

Moment calibration ± 3% of moment reading

Since the moment term, which is subtracted from the lift reading to get the true lift (see Appendix A) is typically about 1/3rd of the lift reading, a total error of ± 9% of the true lift results.

5.4 Drag

The main sources of error were those of trace reading and interaction from lift. The wing tests gave minute deflections at maximum sensitivity and (indeed because) the interaction from lift was considerable. For the cone tests both these factors were better and hence the accuracies are different for the two cases.

For/

For the run considered in para. 5.3 above and a similarly typical cone test corresponding to an incidence of $22\frac{1}{2}°$, the following maximum errors have been calculated.

	Cone	Wing
Trace reading	± 2%	± 27%
Calibration of drag	± 2%	± 2%
Calibration of interaction	± 3%	± 3%
Lift error (used in interaction)	± 5%	± 5%

The interaction corrections are additive and are typically 1/10th and 4 times the drag readings respectively and thus the errors as a percentage of the final drag are ± 5% and ± 12% for cone and wing tests respectively.

5.5 Lift/drag ratio

The possible error for L/D, for small errors, is the sum of the component errors, giving ± 21% for the wing results. When the % error is not small (i.e., near zero lift) this figure can be much increased.

5.6 Centre of pressure position

The accuracy obtainable in centre of pressure position measurement is shown in Appendix C to be given by

$$\frac{\Delta x}{L} = \left(\frac{\Delta M}{M} + \frac{\Delta L'}{L'} \right) \frac{x(x+a)}{aL}$$

with notation as listed and shown in Fig. 1(b).

The dominant effect of the distance of the centre of pressure from the moment sensor datum is evident.

The above expressions together with the errors for lift and moment given before, gives accuracies of ± 0·25% for the cone tests and ± 13% for the wing tests.

5.7 Tunnel running conditions

Measurements of tunnel conditions were not made for each run. A repeatability of 3% over 6 runs was achieved during calibration. Since these runs included instrumentation errors the tunnel repeatability would be expected to be better than 3%.

6. Conclusions

The lift, drag and pitching moment of a 20° half-angle cone and two thin delta wings of triangular and caret cross section have been measured with a strain gauge balance in the Imperial College gun tunnel.

The/

The results of the measurements on the cone agree with previously published data to within ± 5% in lift and ± 3% and ± 1% in drag and centre of pressure position respectively.

The measured values of wing lift, drag, and lift drag ratio agreed well with theoretical estimates based on the two-dimensional oblique shock relationships and laminar skin friction. Newtonian theory with laminar skin friction included gave good estimates of lift/drag ratio though poor estimates of lift and drag.

A maximum lift drag ratio of about 3·7 was obtained for both wings. The slightly greater skin friction drag of the caret wing appeared to be approximately balanced by a slightly higher lift.

Achnowledgements

The work reported here was carried out under a contract from the Science Research Council (formerly D.S.I.R.) and monitored by Dr. L. Pennelegion of the National Physical Laboratory.

Thanks are also due to my Supervisor, Mr. J. L. Stollery, to other members of staff and of the workshop of Imperial College who have helped in various ways and to several members of the Aerodynamics Department, R.A.E., Farnborough, for their constructive comments.

Notation/

Notation

a	Distance from moment datum to L hinge
a'	" " " " " L "
b	a' - a (Fig. 16 and Appendix C)
c_L	Lift coefficient
c_D	Drag coefficient
D	Drag
d	Drag bridge signal
K_L	L bridge constant
$K_{L'}$	L' bridge constant
ℓ	Length of body
l	Signal from L bridge
l'	Signal from L' bridge
L	Lift when used generally
L_1	Symbol for front lift cantilever
L'	Symbol for rear lift cantilever
L_T	True lift. Sometimes lift as determined from L cantilever
$L_{T'}$	Lift as determined from L' cantilever
M_N	Mach number
M	Moment about datum (Fig. 16)
m	Signal from moment bridge
p	Static pressure
R_N	Reynolds number
S	Wing area projected perpendicular to upper ridge line
T_L, T'_L	Loads in appropriate flexure hinges (Appendix B and C)
V	Volume of vehicle
x	Distance from moment datum to centre of pressure
α	Wing incidence. The angle between the free stream and the model centre line; lower centre line for wings
δ^*	Boundary-layer displacement thickness
θ	Angle between shock wave and free stream

References/

References

No.	Author(s)	Title, etc.
1	D. A. Needham	Progress report on the Imperial College Hypersonic Gun Tunnel. Imperial College of Science and Technology, Aeronautics Dept., Tech. Note No.118. August, 1963.
2	S. F. Hoerner	Fluid-Dynamic Drag. Published by the author - 148, Busteed Drive, Midland Park, N.J., U.S.A. 1958.
3	W. R. Wells and W. O. Armstrong	Tables of aerodynamic coefficients obtained from developed Newtonian expressions for complete and partial conic and spheric bodies at combined angles of attack and sideslip with some comparisons with hypersonic experimental data. N.A.S.A. TR R-127. 1962.
4	C. L. Ladson and T. A. Blackstock	Air-helium simulation of the aerodynamic force coefficients of cones at hypersonic speeds. N.A.S.A. TN D-1473. October, 1962.
5	J. A. Penland	Aerodynamic force characteristics of a series of lifting cone and cone-cylinder configurations at a Mach number of 6·83 and angles of attack up to 130°. N.A.S.A. TN D-840. June, 1961.
6	J. A. Penland	A study of the stability and location of the centre of pressure on sharp, right circular cones at hypersonic speeds. N.A.S.A. TN-2283. May, 1964.
7	-	Equations, tables, and charts for compressible flow. Ames Research Staff. N.A.C.A. Report 1135. 1953.
8	R. J. Monaghan	An approximate solution of the compressible laminar boundary layer on a flat plate. A.R.C. R. & M. 2760. November, 1949.
9	D. Catherall	Boundary-layer characteristics of caret wings. A.R.C. C.P. 694 August, 1962.

10./

No.	Author(s)	Title, etc
10	H. H. King	A tabulation of base flow properties for cones and wedges. Electro-Optical Systems Inc., Report RN - 17. (AD 426983).
11	J. C. Cooke	Leading edge effects on caret wings. R.A.E. Tech. Note Aero.2943. A.R.C.25 840 - F.M.3449 - Hyp.418. January, 1964.
12	L. Pennelegion, G. S. Smith and K. Dolman	Millisecond measurements of aerodynamic forces in a high-pressure shock tunnel. NPL Aero Report 1120. A.R.C.26 309 - Hyp.451. October, 1964.
13	C. H. McLellan, M. H. Bertram and J. A. Moore	An investigation of four wings of square plan form at a Mach number of 6·9 in the Langley 11-inch hypersonic tunnel. N.A.C.A. Report 1310. 1957.
14	J. R. Martin, G. R. Duryea and L. M. Stevenson	Instrumentation for force and pressure measurements in a hypersonic shock tunnel. Proceedings of Second Symposium on Hypervelocity Techniques, University of Denver, 20-21st March, 1962. Plenum Press, N.Y.
15	A. S. Platov and H. A. Ricci	Wind tunnel tests of solid state strain gauges. Proceedings of the 1st International Congress on Instrumentation in Aerospace Simulation facilities, L'Ecole Nationale Superieure de l'Aéronautique, Paris. September, 1964.
16	D. A. Babaev	Numerical solution of the problem of supersonic flow past the lower surface of a delta wing. A.I.A.A. Journal Vol. 1, p. 2224 - 2231. September, 1963.
17	J. Becker	Studies of high lift/drag ratio hypersonic configurations. International Council of the Aeronautical Sciences, 4th Congress, Paris, 24-28th August, 1964. ICAS Paper No. 64-551.
18	T. A. Blackstock and C. L. Ladson	Comparison of the hypersonic aerodynamic characteristics of some simple winged shapes in air and helium. N.A.S.A. TN D-2328. June, 1964.
19	L. C. Squire	Pressure distributions and flow patterns at M = 4·0 on some delta wings. A.R.C. R. & M. 3573. February, 1963.

APPENDIX A/

APPENDIX A

Balance Calibrations

1. Calibrations Made

Several calibrations were carried out before, during and after the series of tests described in this report using different instruments and techniques. They are enumerated below.

(a) Before the series of tests commenced, a complete calibration including interactions was carried out using a Solartron digital voltmeter type LM 10102 as the test instrument. Checks were also made using an oscilloscope of the type used in operation (Tektronix 502) with and without the D.V.M. connected.

(b) A dynamic check on the drag interaction was made by dropping weights from the balance and recording the apparent drag changes on an oscilloscope.

(c) In situ calibrations of the lift and moment and the drag interaction were carried out before and several times during the wing tests. These were made by using a slow scan rate on the C.R.O. and lifting the weights rapidly on and off the balance.

(d) Some time after the conclusion of the tests covered by this report a further complete calibration was carried out using a Digital Measurement D.V.M.

(e) After preliminary tests with some further wings (during which high overshoot loads were encountered) the drag sensor was changed to silicon gauges and a further complete re-calibration carried out using a Solartron D.V.M. type LM 1420.

(f) Finally, in order to try and clear up certain inconsistencies in the calibrations and results, a method was devised of dropping weights consistently from the balance and a dynamic calibration of lift, moment and interaction of lift on drag was carried out.

The results of all the calibrations are shown in Figures A 1 to A 5. Due to having been strained, the balance showed some unusual characteristics and this together with the different circumstances and methods of each calibration was responsible for some of the variation between calibrations, though genuine changes of sensitivity may also have occurred.

2. Moment Channel

This was consistent throughout, though a slight shift of calibration occurred in the interval between the end of the tests described herein and the recalibration preceding the next tests. As seen in Fig. A 1, calibrations (a) and (c) agreed, giving 0·55 lb in./mv for normal temperatures (datum combined resistance reading of 470 = 249·8 Ω). The variation in gauge factor due to temperature was 0·67%/Ω or about 0·4%/°C temperature change.

The/

The later calibrations, (d), (e) and (f) (not shown on the graph for clarity) gave a sensitivity of 0·575 lb in./mv when corrected to the same datum temperature, representing an apparent change in calibration of 4½% in about six months.

3. Drag Channel

The various calibrations are plotted in Fig. A 2. A sensitivity of 6·3 lb/mv was obtained.

4. Lift Channels

These channels showed the greatest variation. The results for the forward lift cantilever (designated L_1) are plotted in Fig. A 3 and those for the rear cantilever (designated L') in Fig. A 4.

The initial calibration of the L_1 channel was non-linear and appeared to give a slightly different non-linear line for each position of the centre of pressure. The mean line chosen did not pass through the origin and was given by

$$\text{Lift} = 1{\cdot}85 \times \text{mv reading} - 0{\cdot}2 - \frac{M}{6} \text{ lb}$$

where M is the moment of lift about the moment datum and 0·2 lb was the amount by which the chosen line did not pass through the origin.

The calibrations (c) made during the last set of the present tests confirmed this value but later calibrations (d), (e), (f) tended away from this to a minimum value of 1·65 instead of 1·85 and with the final dynamic calibration being somewhere between the two extremes.

The initial calibration of the L' channel was similar in form to the L_1 channel and the chosen line gave:-

$$\text{Lift} = 3{\cdot}03 \times \text{mv reading} - 0{\cdot}2 - \frac{M}{3} \text{ lb.}$$

The calibrations (c) gave a slightly different result:-

$$\text{Lift} = 3{\cdot}12 \times \text{mv reading} - \frac{M}{3} \text{ lb}$$

and this was used for the wing tests. Subsequent calibrations lay between the two above values. Both lift channels exhibited hysteresis and the L' channel at high loads took a finite time (about 50 m sec) to fully return to its zero (as shown by the dynamic calibrations).

To summarize, although the calibration constants of the lift channels varied slightly with time and use, the variation through the test period was small, as shown by frequent calibrations (< 5%).

Subsequent calibrations showed continued variations but also showed that, at least for times greater than 50 m sec there was no difference between static and dynamic results.

5./

5. Interactions

All interactions other than that of lift on drag were negligible. The interaction of lift on drag is plotted in Fig. A 5. The initial calibration shows the hysteresis, mainly of the loading system. The mean, of 11·4% of the L' sensor reading, coincided with that obtained by dropping a weight from the balance (calibration (b)). However, three checks carried out during the wing tests (calibration (c)), each gave a value of 10% and this was used for these tests. Calibration (d), sometime after the tests again gave 11·4%. For later calibrations this channel had been changed to silicon gauges.

Also plotted in Fig. A 5 is a residual correction used for the cone results which corrected the chosen straight line to the non-linear line for the appropriate centre of pressure position.

Note: All the sensitivities quoted are for 9v basic excitation voltage (i.e., 3v on moment channel).

6. Deflections under Load

For the cone tests the incidence deflection for maximum load was 0·1°. For the wing tests it was 0·13°/lb which was allowed for, in addition to incidence measurements from the schleiren photographs.

APPENDIX B/

APPENDIX B

Method of Obtaining Lift Measurement

The lift may be obtained from any two of the three readings, front lift, rear lift and moment. It is more accurate to take either lift reading with the moment.

With the notation as listed and shown in Fig. 1(b), taking moments about the moment datum,

$$M + aT_L - a'T'_L = 0 \qquad \ldots(B.1)$$

and

$$L + T'_L - T_L = 0 \qquad \ldots(B.2)$$

substituting (B.2) into (B.1), rearranging, and noting that $L \equiv L_T$ when derived from T_L or $L \equiv L'_T$ when derived from T'_L,

$$L'_T = \left(\frac{a'}{a} - 1\right) T'_L - \frac{M}{a} \qquad \ldots(B.3)$$

or

$$L_T = \left(1 - \frac{a}{a'}\right) T_L - \frac{M}{a'}. \qquad \ldots(B.4)$$

Hence plotting $L + \frac{M}{a'}$ or $L + \frac{M}{a}$ against ℓ or ℓ' respectively will produce a straight line whose slope is $k_L\left(1 - \frac{a}{a'}\right)$ or $k'_L\left(\frac{a'}{a} - 1\right)$ respectively, where $k_L \propto T_L$ and $k'_L \propto T'_L$.

These values are plotted in Figs. A.3 and A.4.

APPENDIX C/

APPENDIX C

Derivation of Balance Accuracy Estimation

1. Lift/Drag Ratio

$$\Delta\frac{L}{D} = \frac{\partial\, L/D}{\partial L}\Delta L \pm \frac{\partial\, L/D}{\partial D}\Delta D$$

$$= \frac{1}{D}\Delta L + \frac{L}{D^2}\Delta D$$

$$\therefore \frac{\Delta\, L/D}{L/D} = \frac{\Delta L}{L} + \frac{\Delta D}{D}.$$

2. Centre of Pressure Position

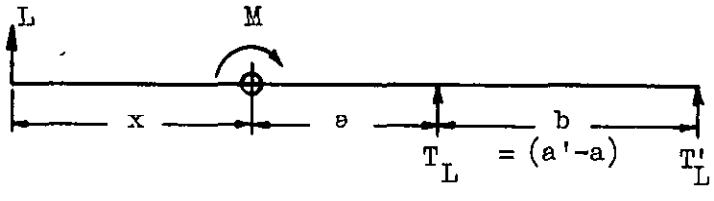

$$x = \frac{M}{L} \qquad \ldots(C.1)$$

$$\therefore \Delta x = \frac{\partial x}{\partial M}\Delta M \pm \frac{\partial x}{\partial L}\Delta L$$

$$= \frac{\Delta M}{L} + \frac{M}{L^2}\Delta L. \qquad \ldots(C.2)$$

Therefore from (C.1)

$$\frac{\Delta x}{x} = \frac{\Delta M}{M} + \frac{\Delta L}{L}. \qquad \ldots(C.3)$$

Similarly, since $$L = \frac{T'_L b}{(x+a)}$$

$$\frac{\Delta L}{L} = \frac{\Delta T'_L}{T'_I} + \frac{\Delta x}{(x+a)}. \qquad \ldots(C.4)$$

Substituting/

Substituting (C.4) into (C.3) and rearranging

$$\frac{\Delta x}{x} = \left(\frac{\Delta M}{M} + \frac{\Delta T_L'}{T_L'}\right)\left(\frac{x + a}{a}\right).$$

The % centre of pressure position for the body under test can be represented by $\frac{\Delta x}{L}$, hence finally, $\frac{\Delta x}{L} \simeq \left(\frac{\Delta M}{M} + \frac{\Delta T_L'}{T_L'}\right)\frac{x(x+a)}{aL}$.

PC
ES

D7692/1/125875 K3 10/66 XL

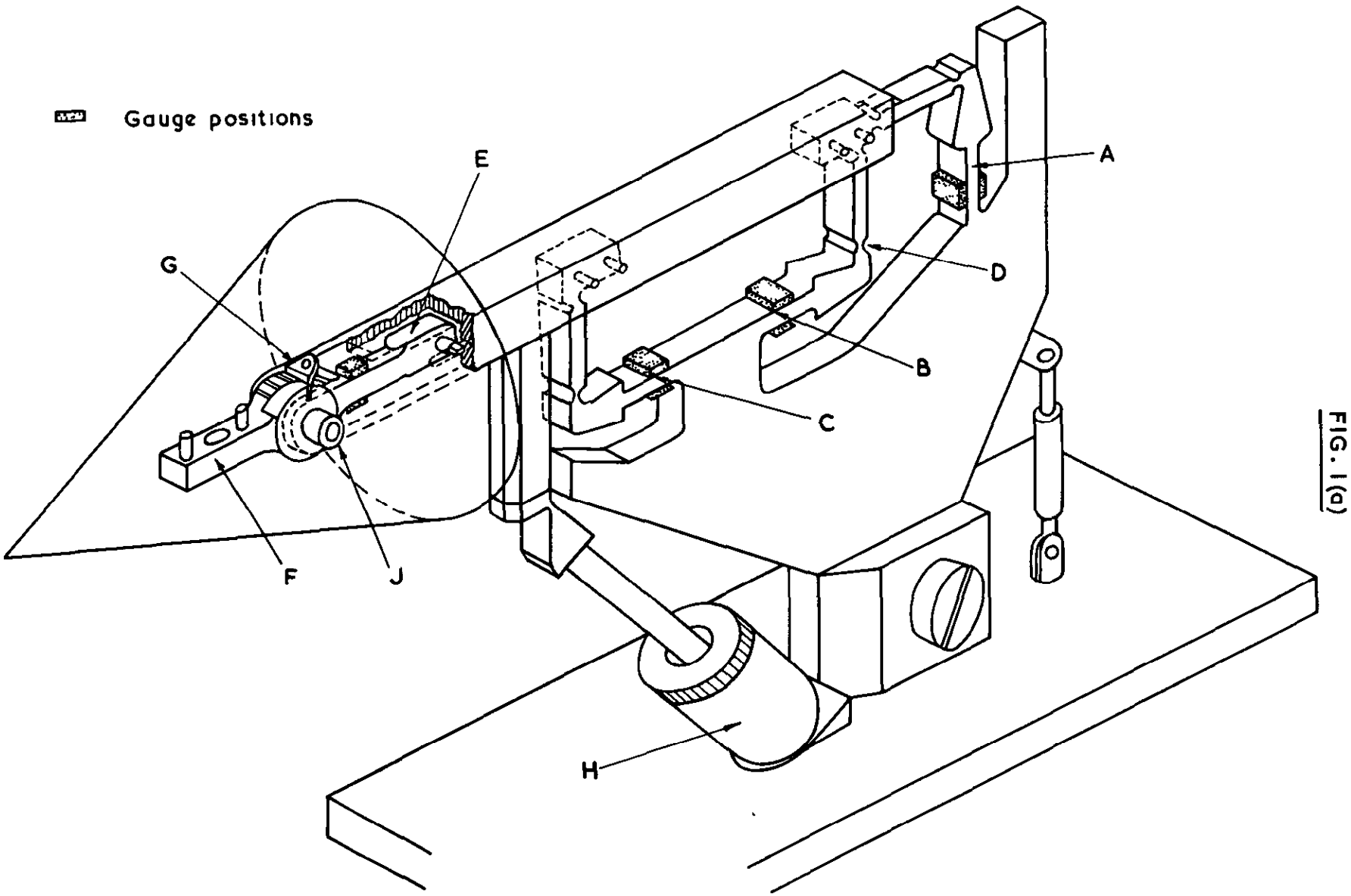

FIG. 1(a)

Layout of balance (Covers off)

FIG. 1(b)

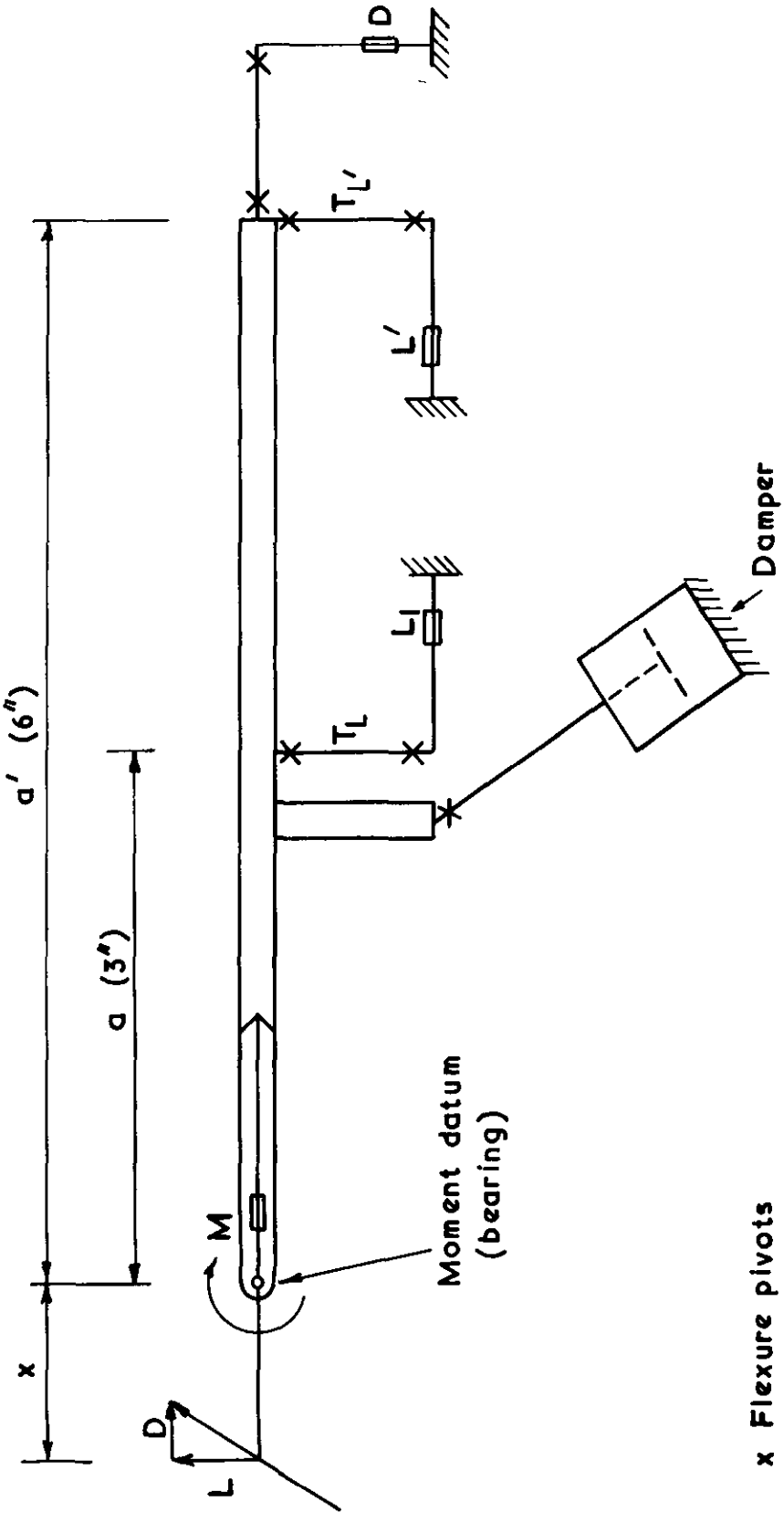

x Flexure pivots

General arrangement of balance

FIG. 2 (a & b)

P_1 = Initial barrel pressure
P_4 = Drive vessel pressure

Drag D

Rear lift L′

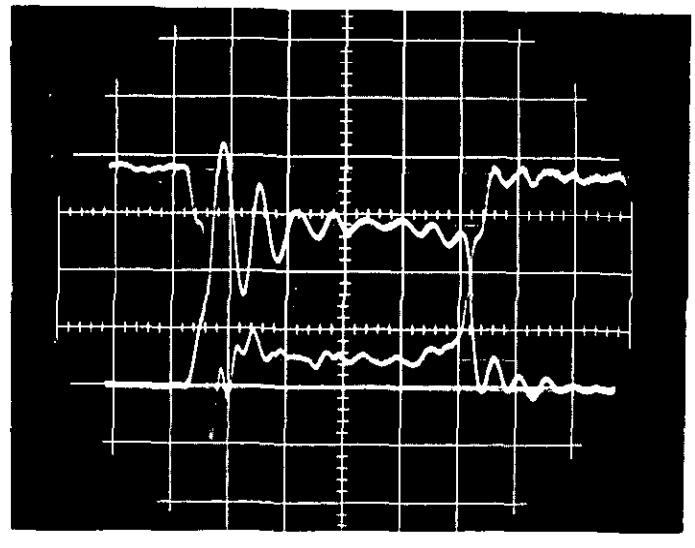

Time base
1 cm = 10 m sec
P_4 = 1000 p.s i.
P_1 = 14 7 p.s.i

(a) With damping (cone model)

Front lift L_1

Rear lift L′

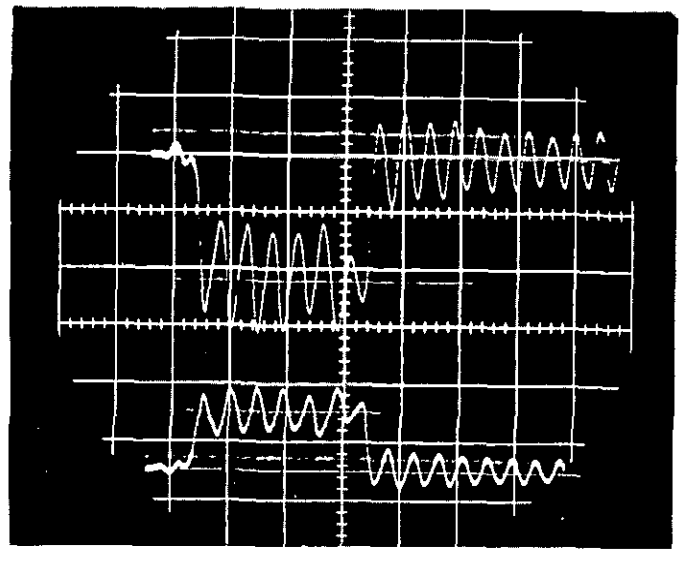

Time base
1 cm = 10 m sec
(Mach 10)
P_4 = 2000 p.s.i
P_1 = 14·7 p.s.i.

(b) Without damping (original balance)

Typical traces with and without damping

FIG.2 (c – e)

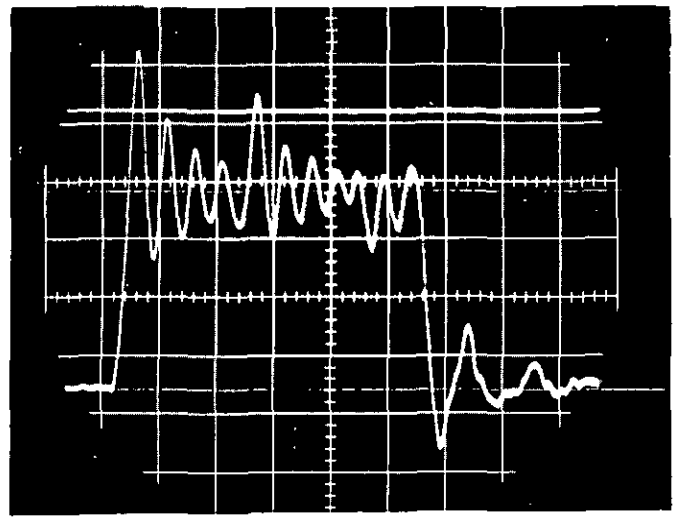

Front lift L_1

Time base
1cm = 20 m sec
P_4 = 1000 p.s i.
P_1 = 40 p.s.i

(c)

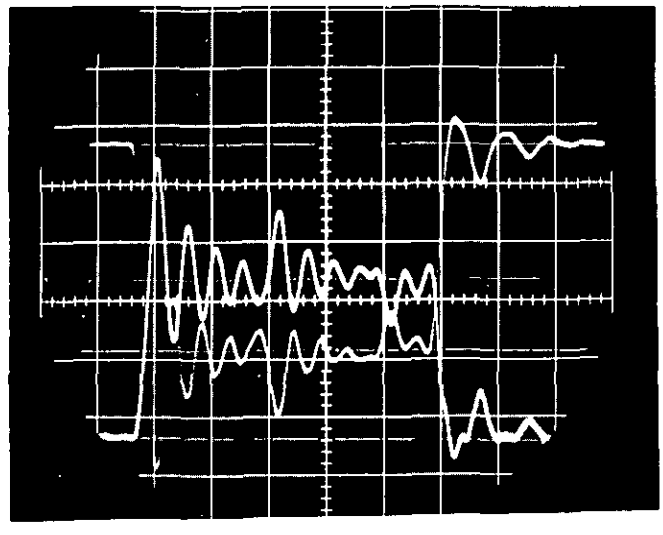

Moment M

Front lift L_1

Time base
1 cm = 20 m sec
P_4 = 1000 p.s i.
P_1 = 40 p.s i

(d)

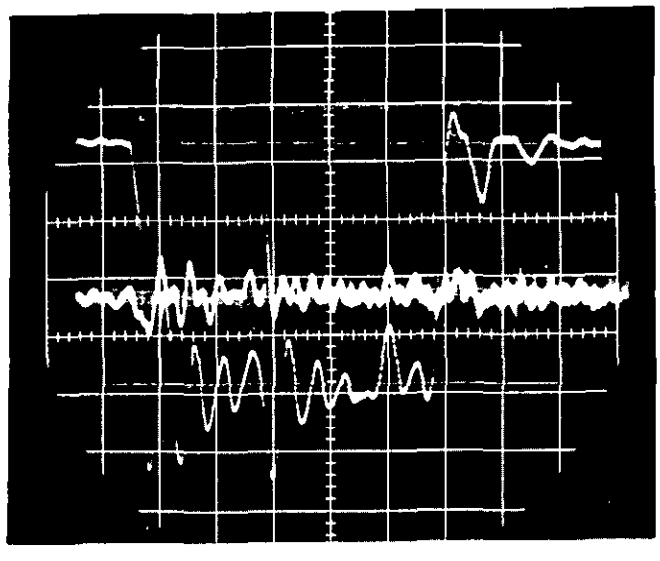

Rear lift L'

Drag D

Time base
1 cm = 20 m sec
P_4 = 1000 p s i
P_1 = 40 p s i

(e)

Typical traces with wing models

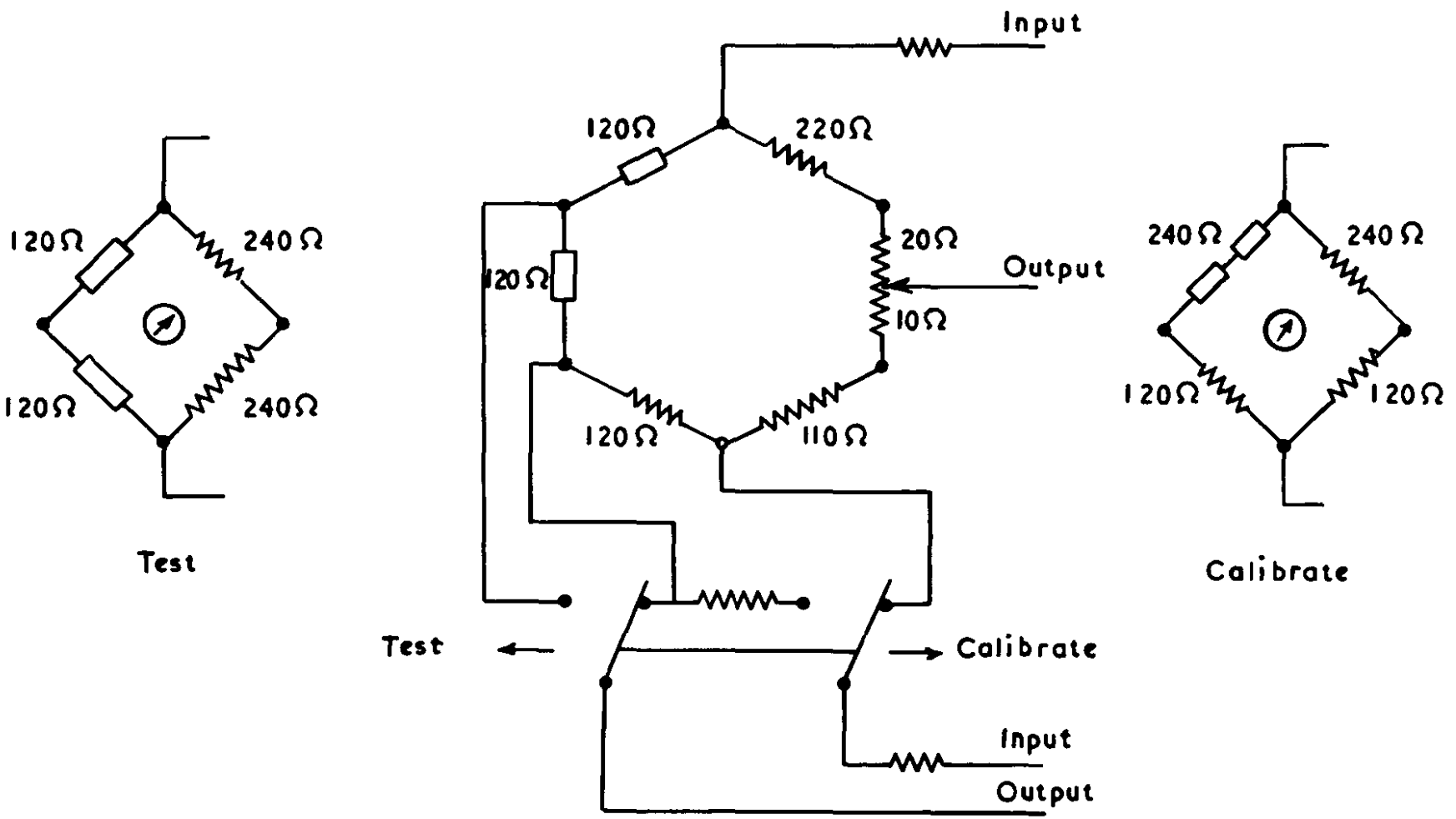

FIG 3

Moment sensor circuit

FIG. 4

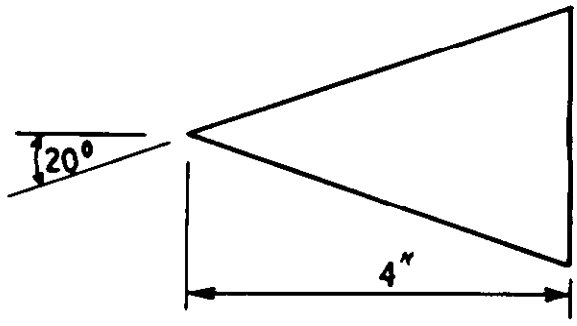

Weight 51 gms.

(a) Cone

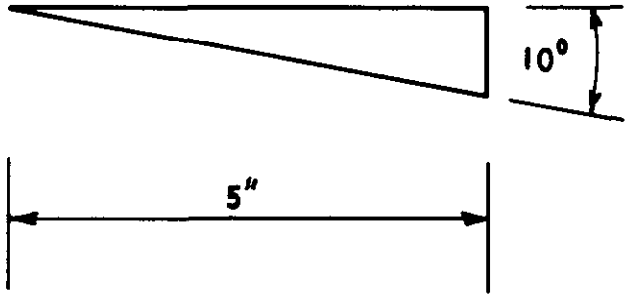

(b) Plain Delta

Both wings

AR = 1

$\frac{V}{S^{3/2}} = 0.116$

Weight = 135 gms.

L.E. thickness
0.004" to 0.007" dia.

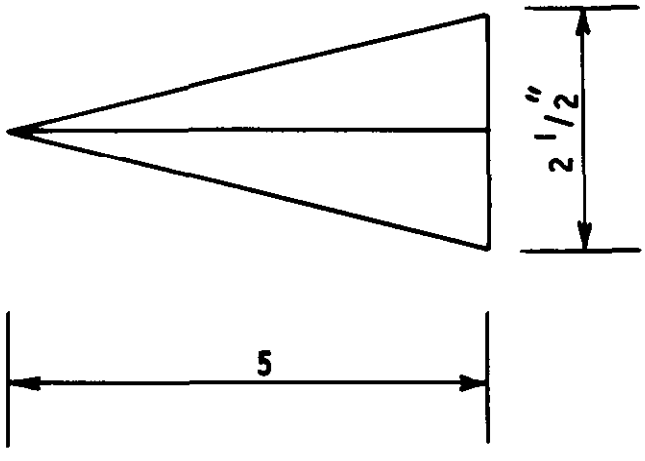

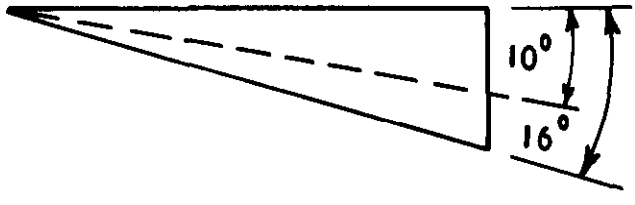

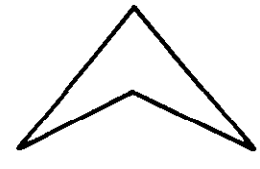

(c) Caret Delta

Sketch of models

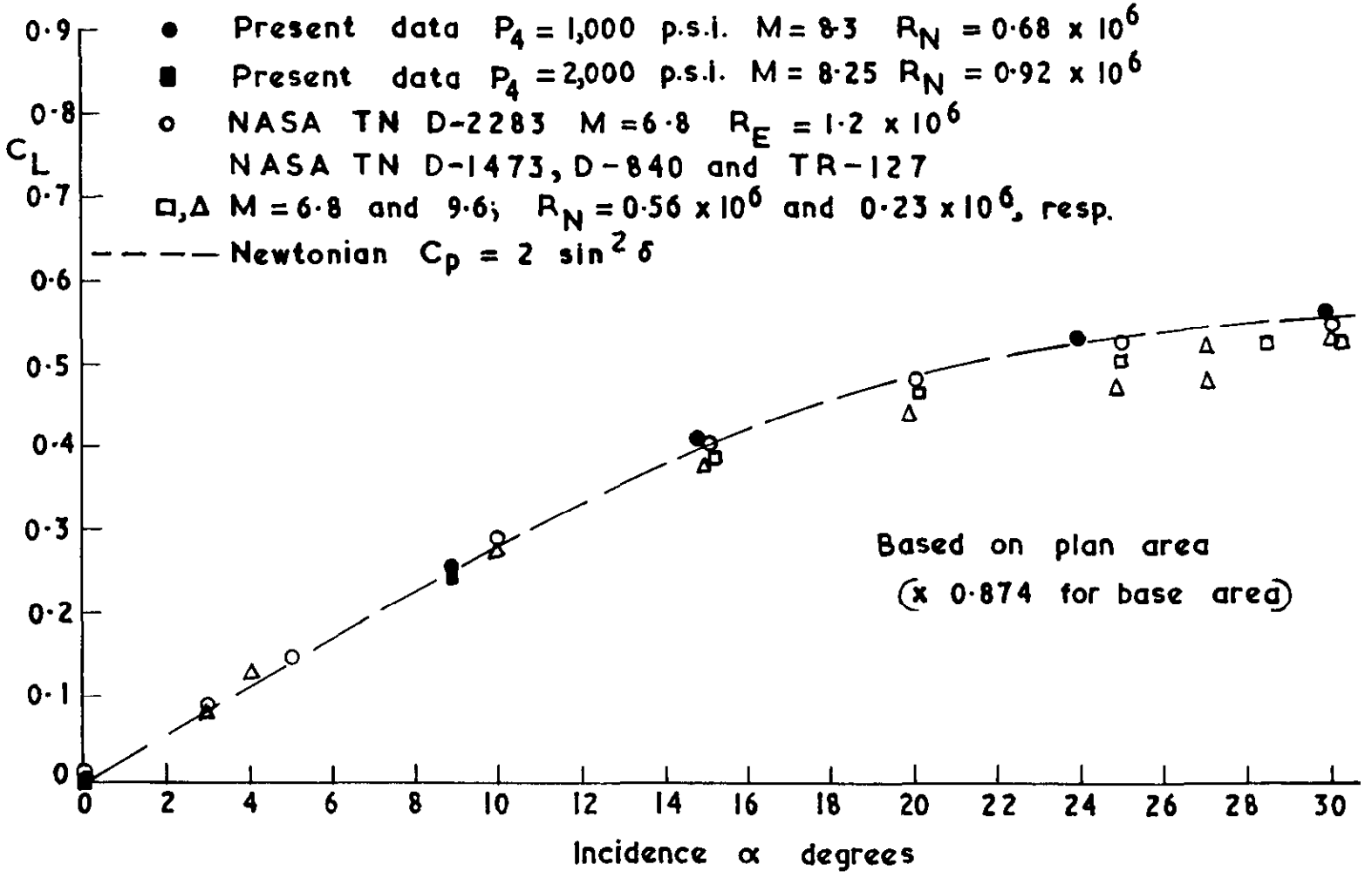

Lift of 20° half angle cone M = 8·3

FIG. 5

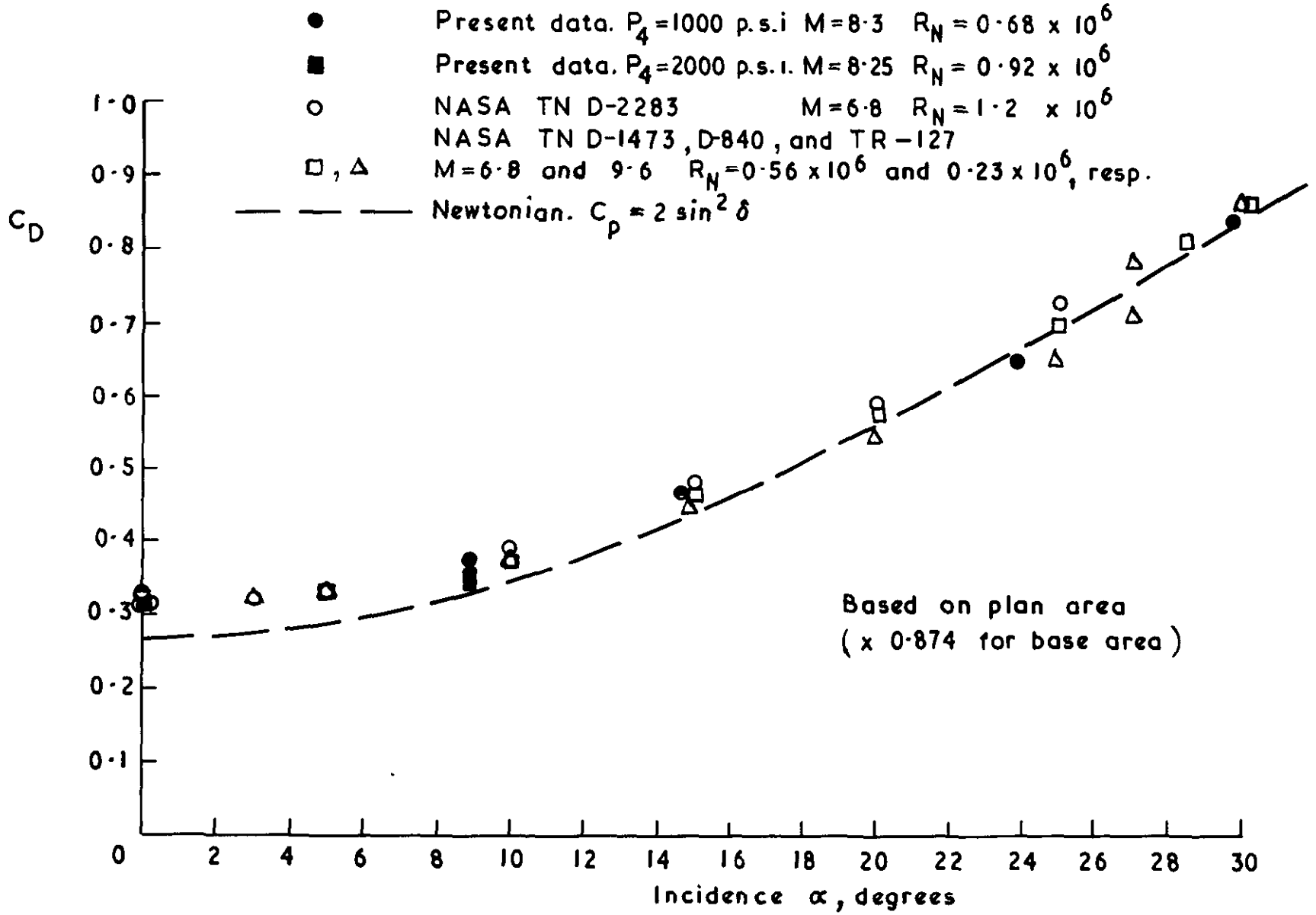

FIG. 6

Drag of 20° half angle cone M = 8·3

FIG. 7

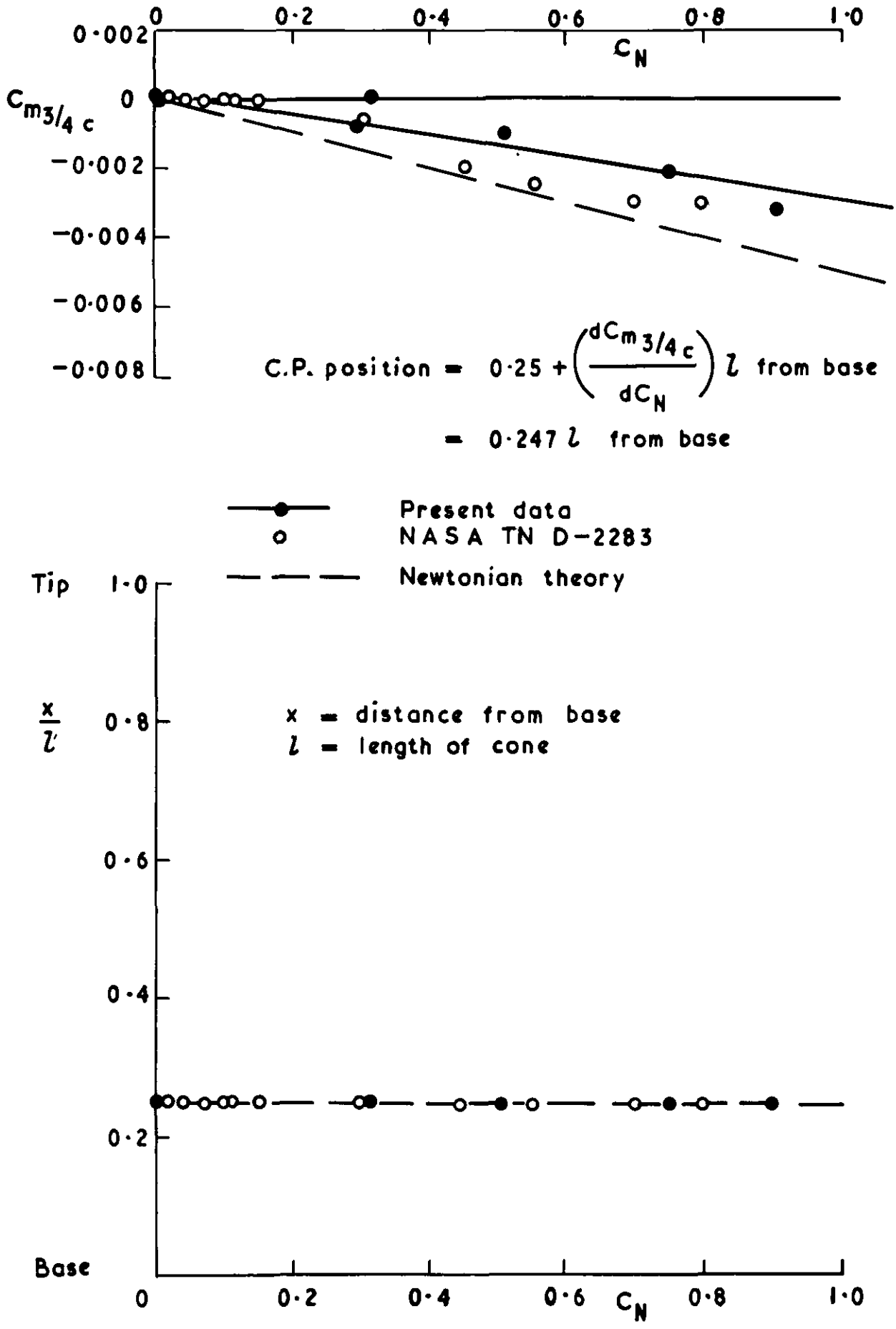

C.P. position on a 20° half angle cone

FIG. 8

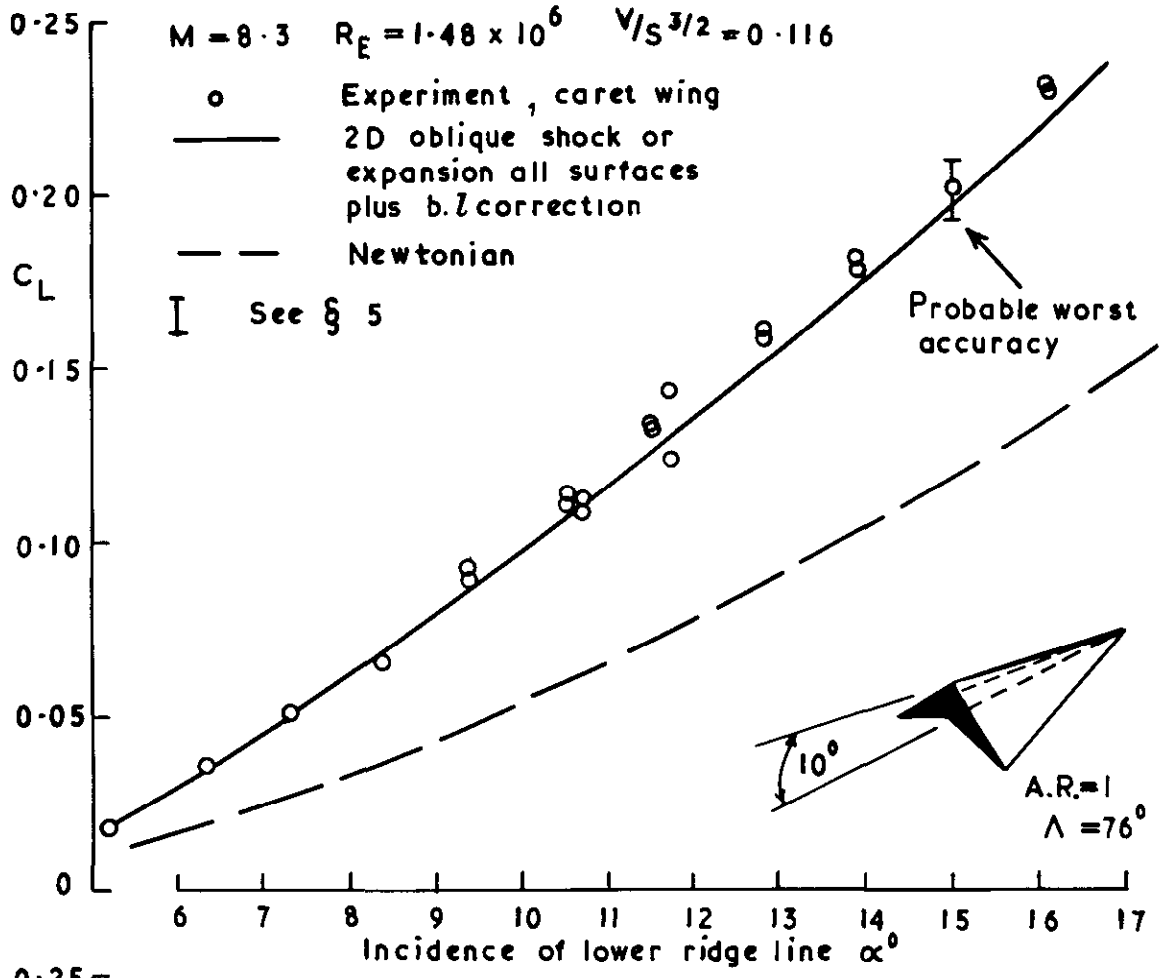

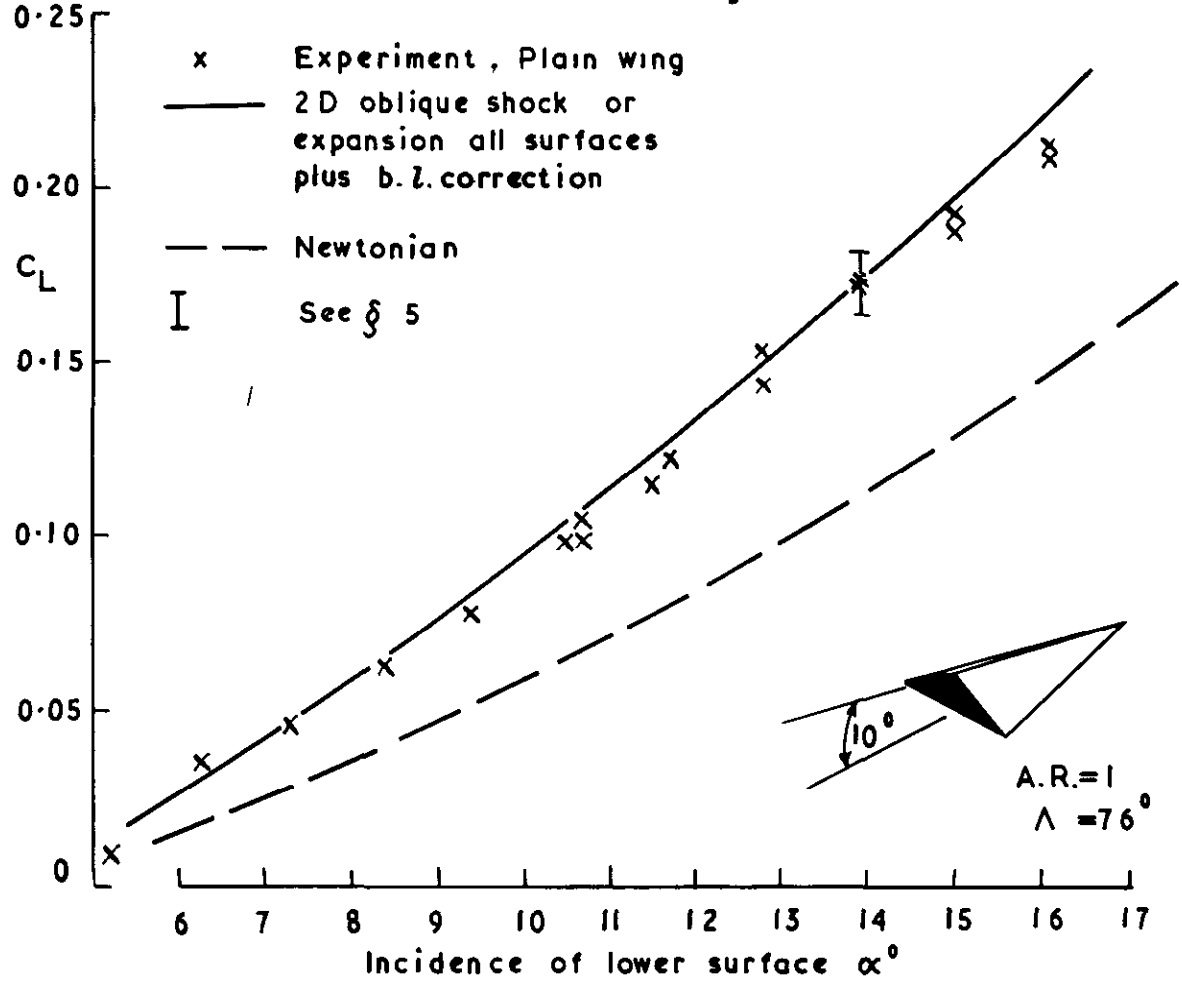

Lift of delta wings

FIG. 9

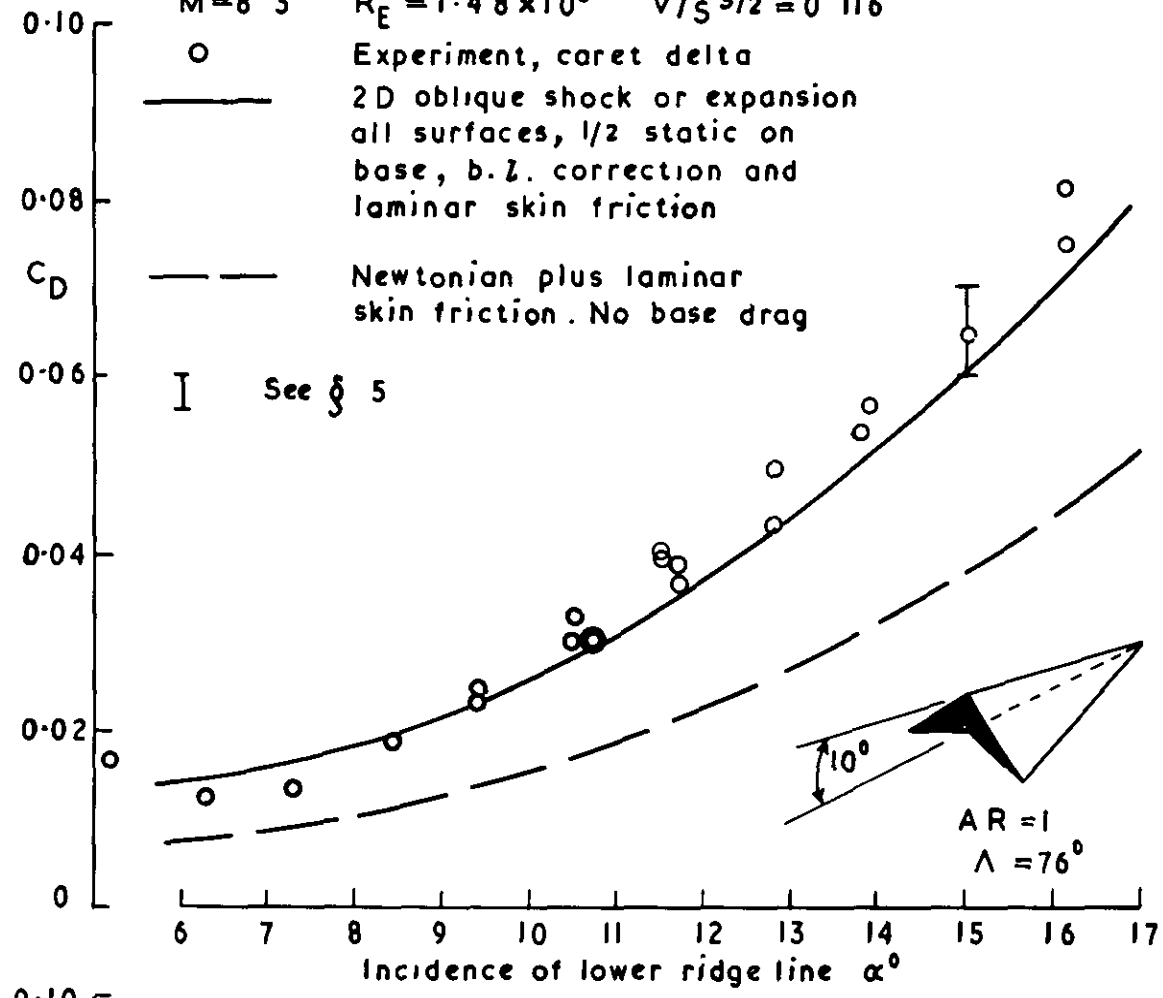

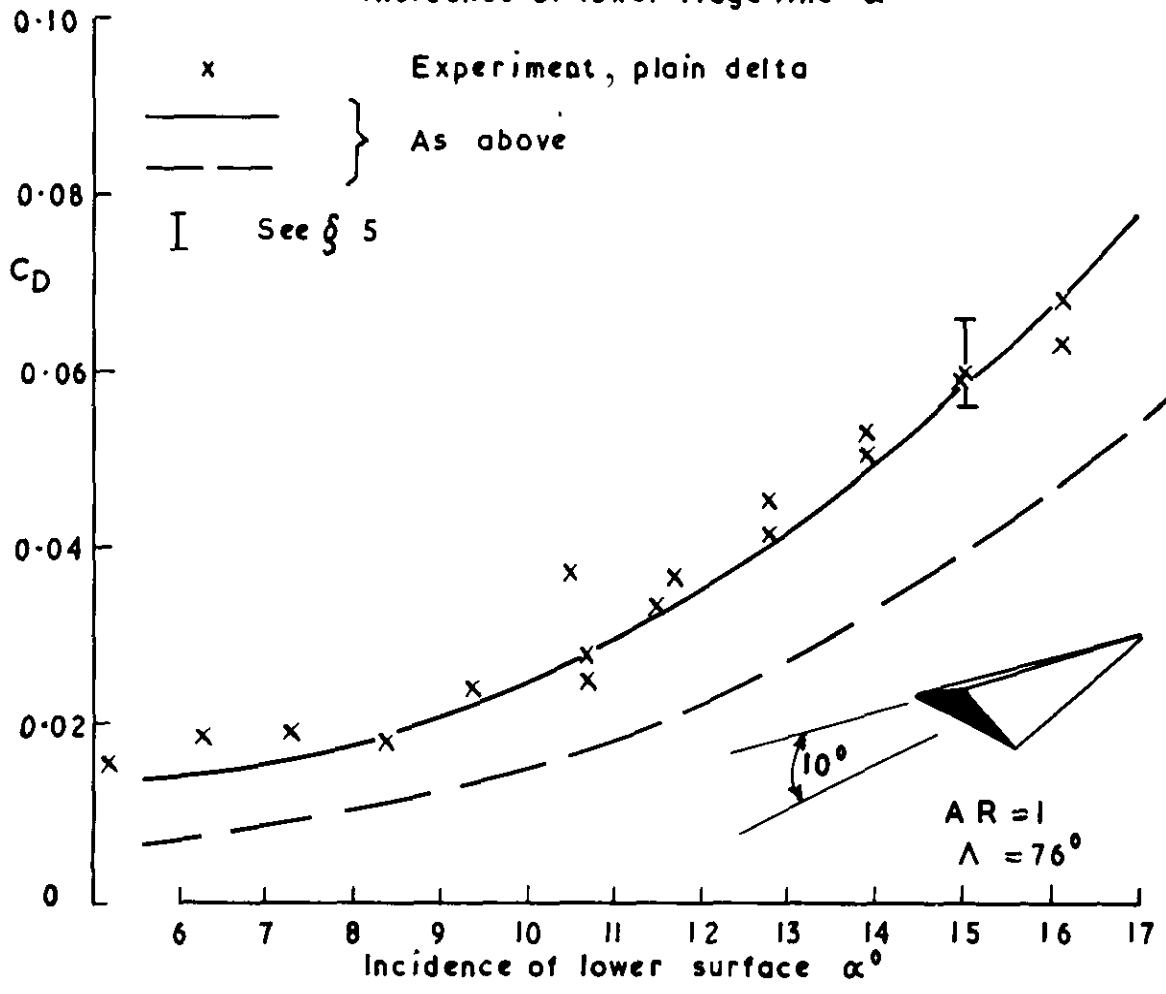

Drag of delta wings

FIG. 10

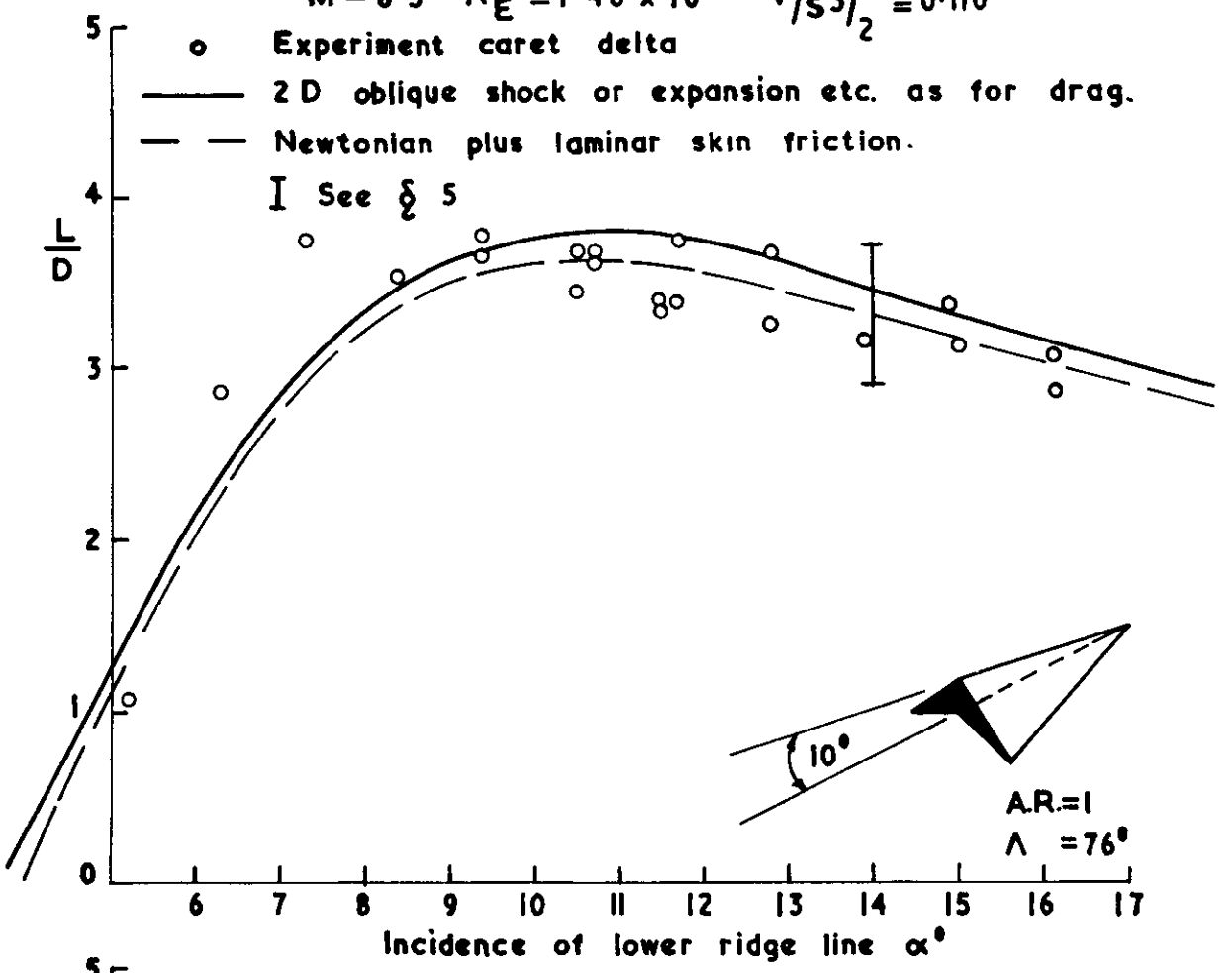

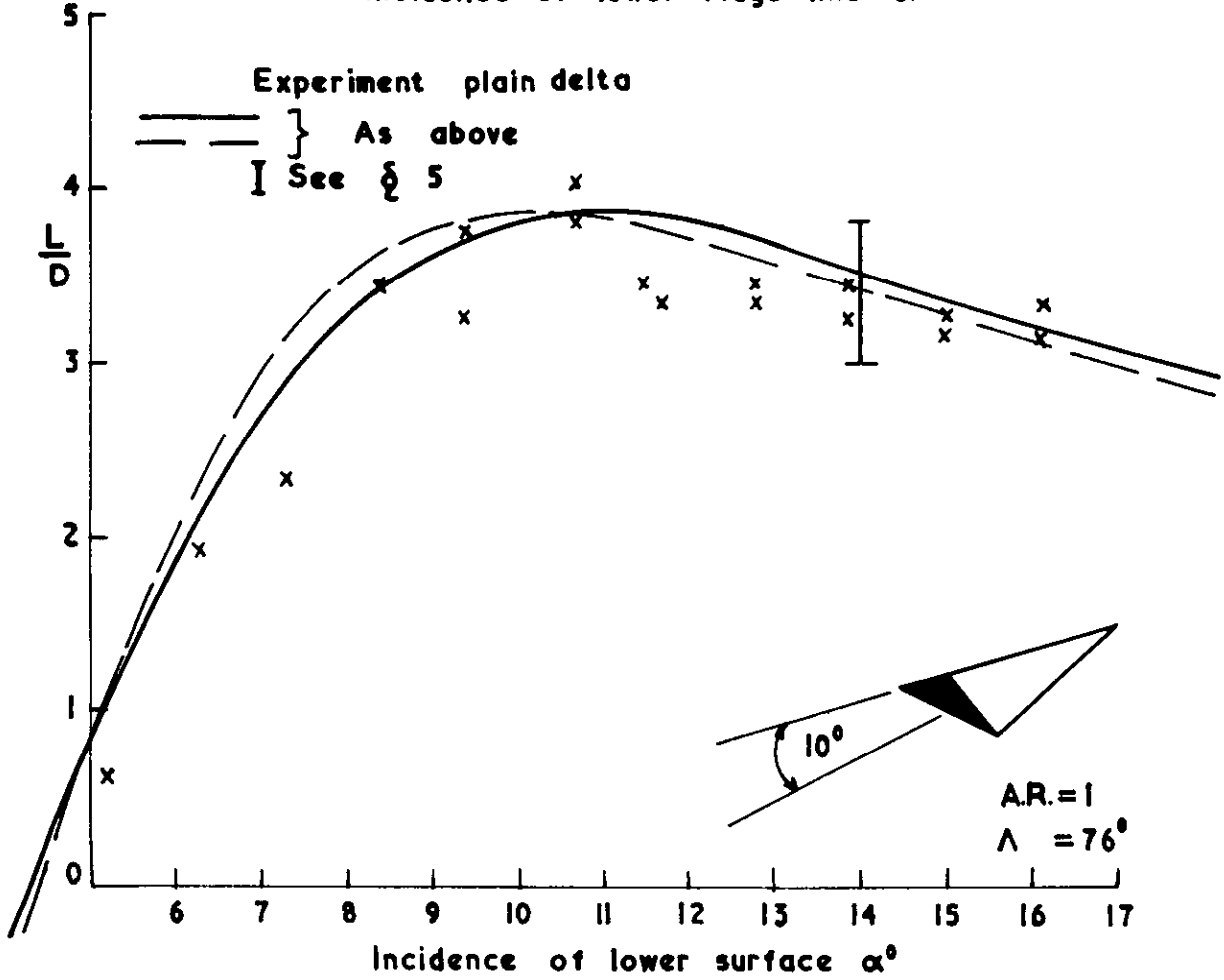

L/D ratio of delta wings

FIG.11

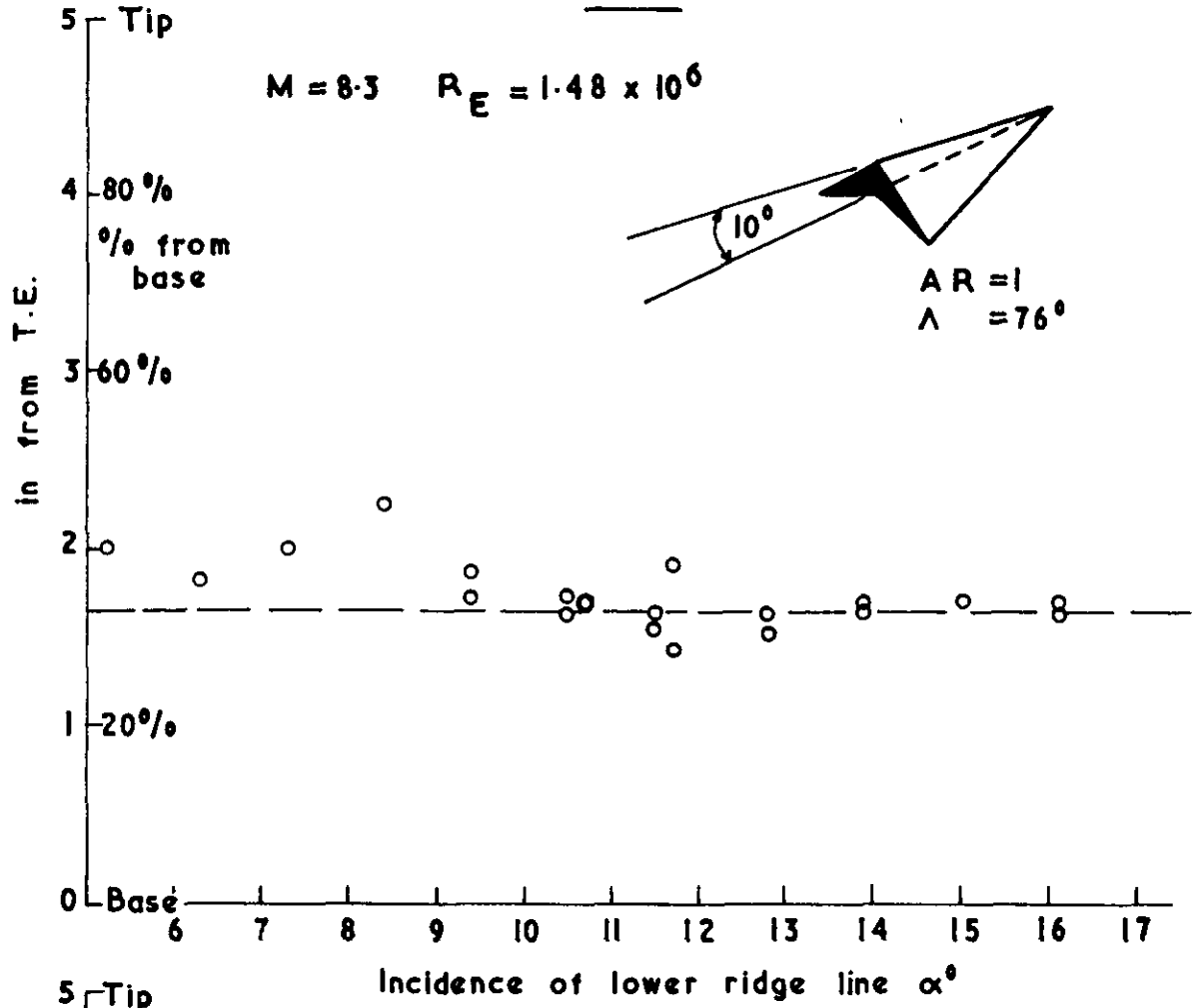

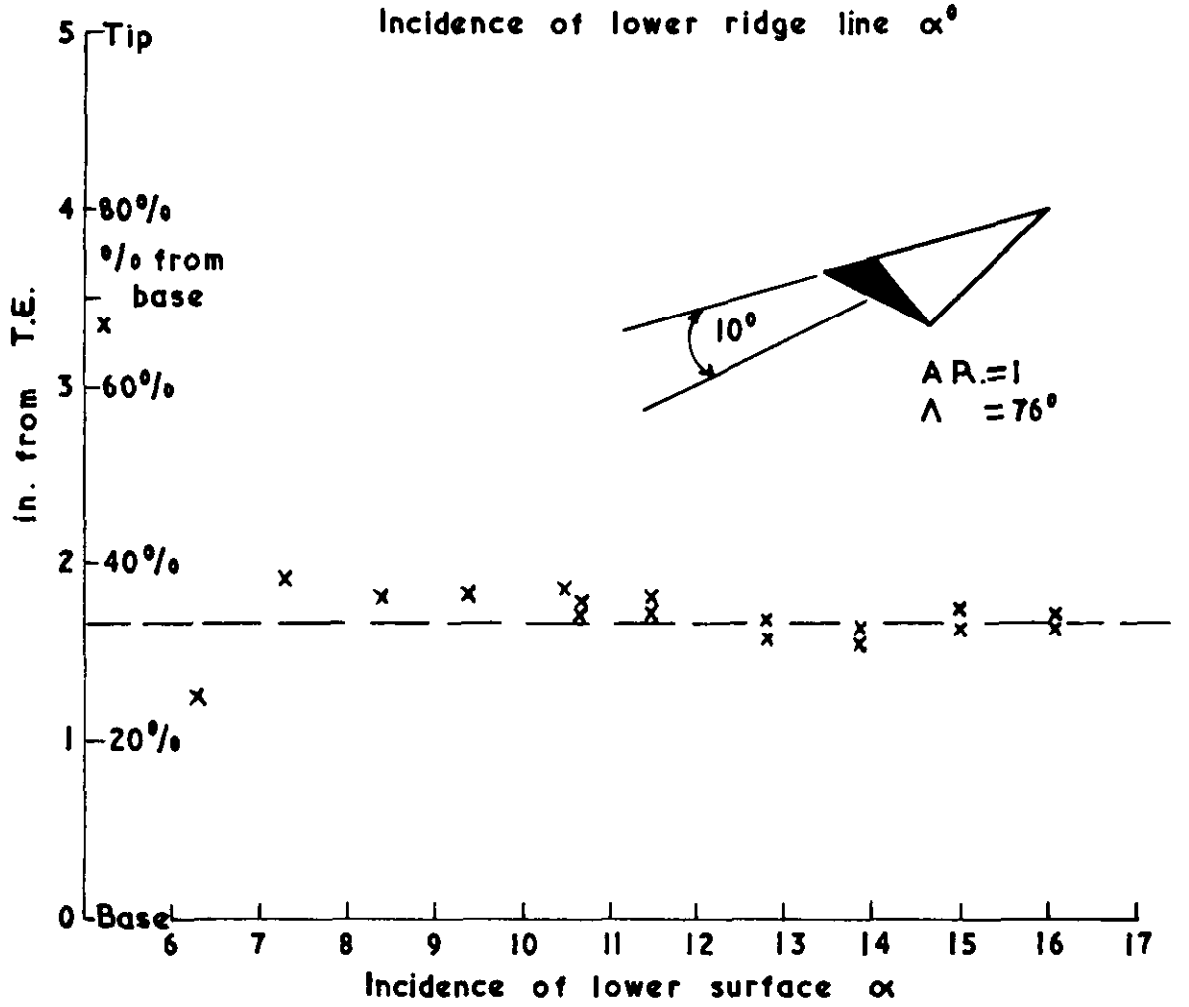

C.P. position on delta wings

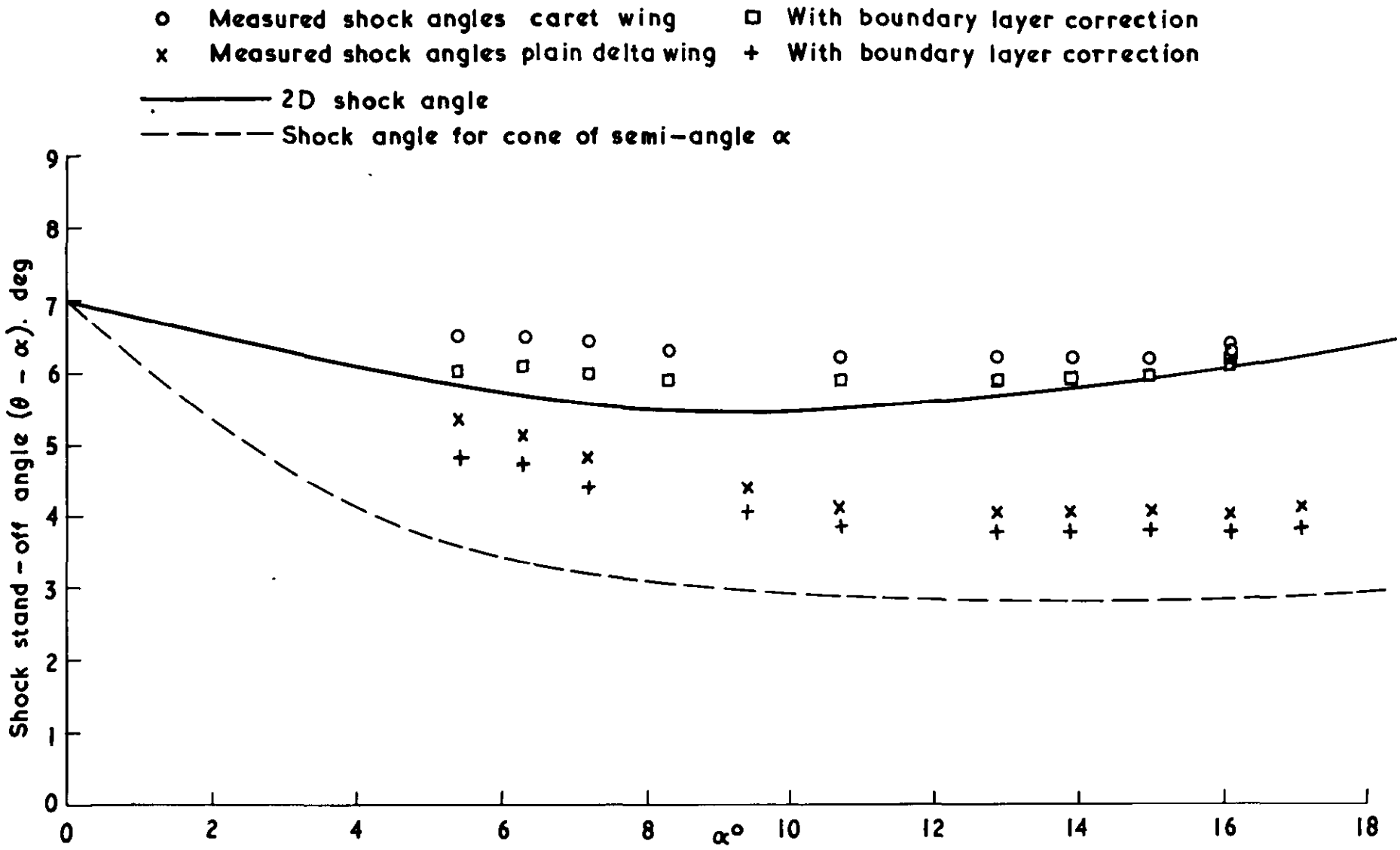

FIG. 12(a)

Shock angles on delta wings

FIG. 12 (b & c)

(b) Plain delta, $\alpha = 10{\cdot}7^0$, $M = 8{\cdot}3$

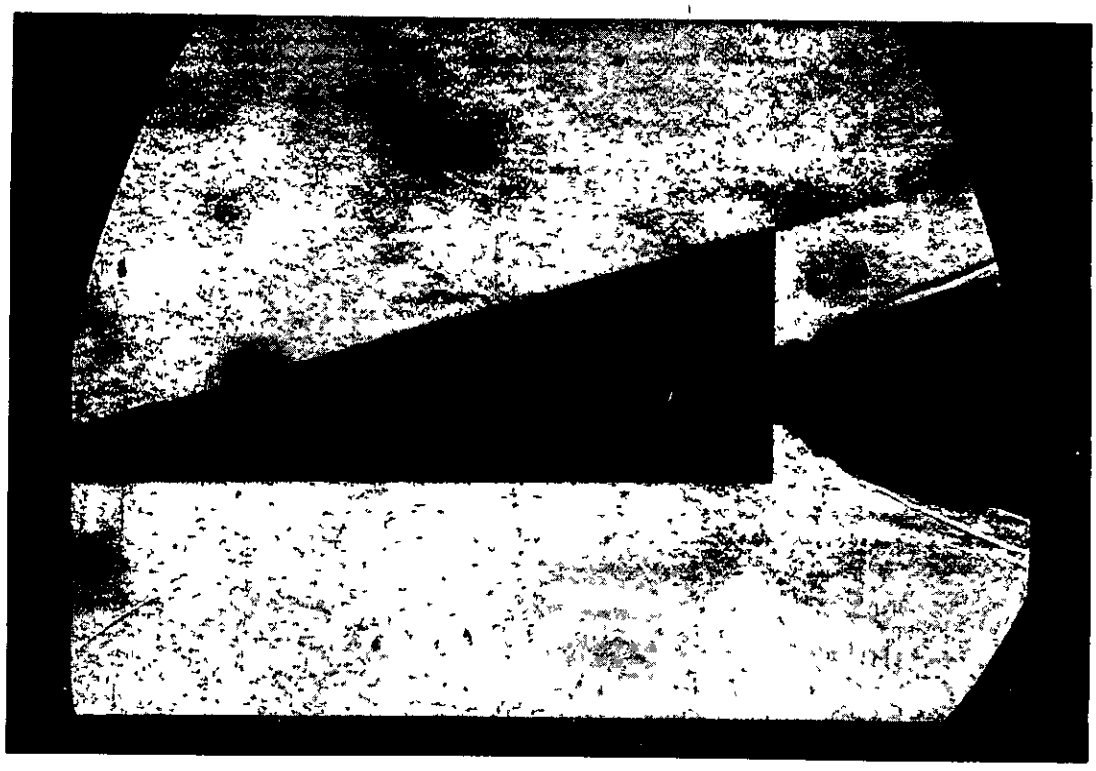

(c) Caret delta, $\alpha = 10{\cdot}3^0$, $M = 8{\cdot}3$

Schlieren of flow (Side view)

FIG 12 (d & e)

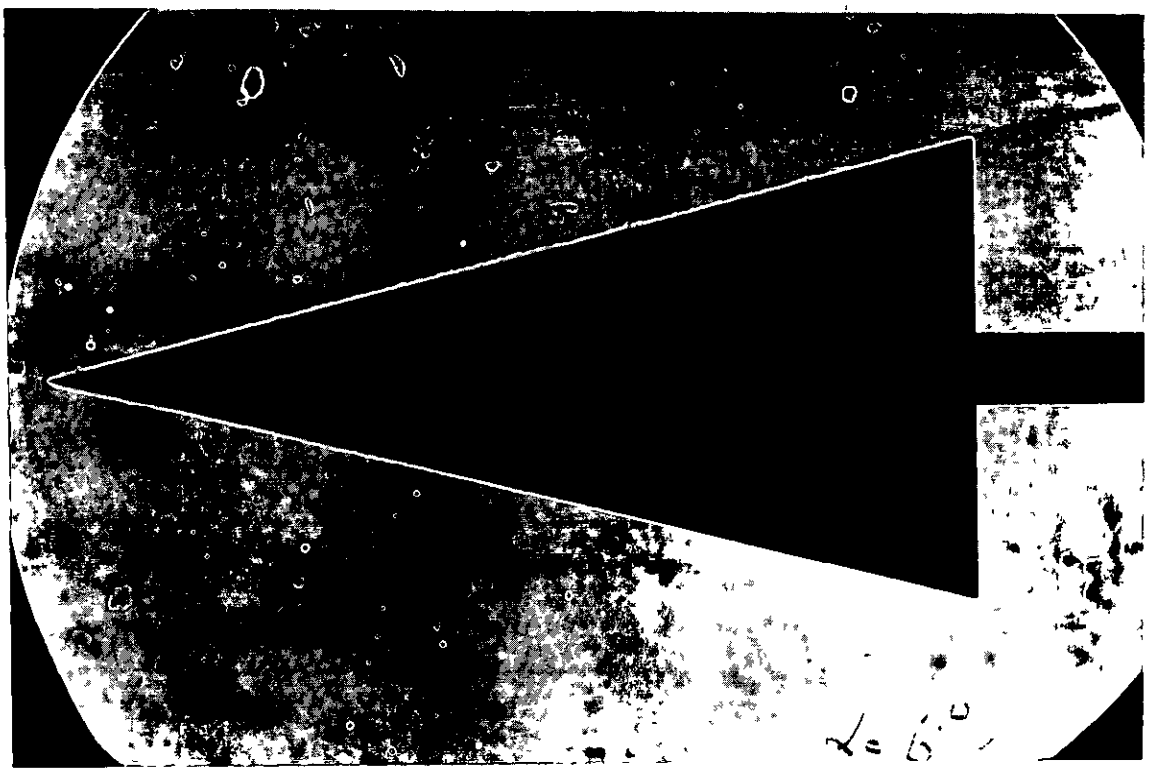

(d) Plain delta, $\alpha = 6^0$, $M = 8{\cdot}3$

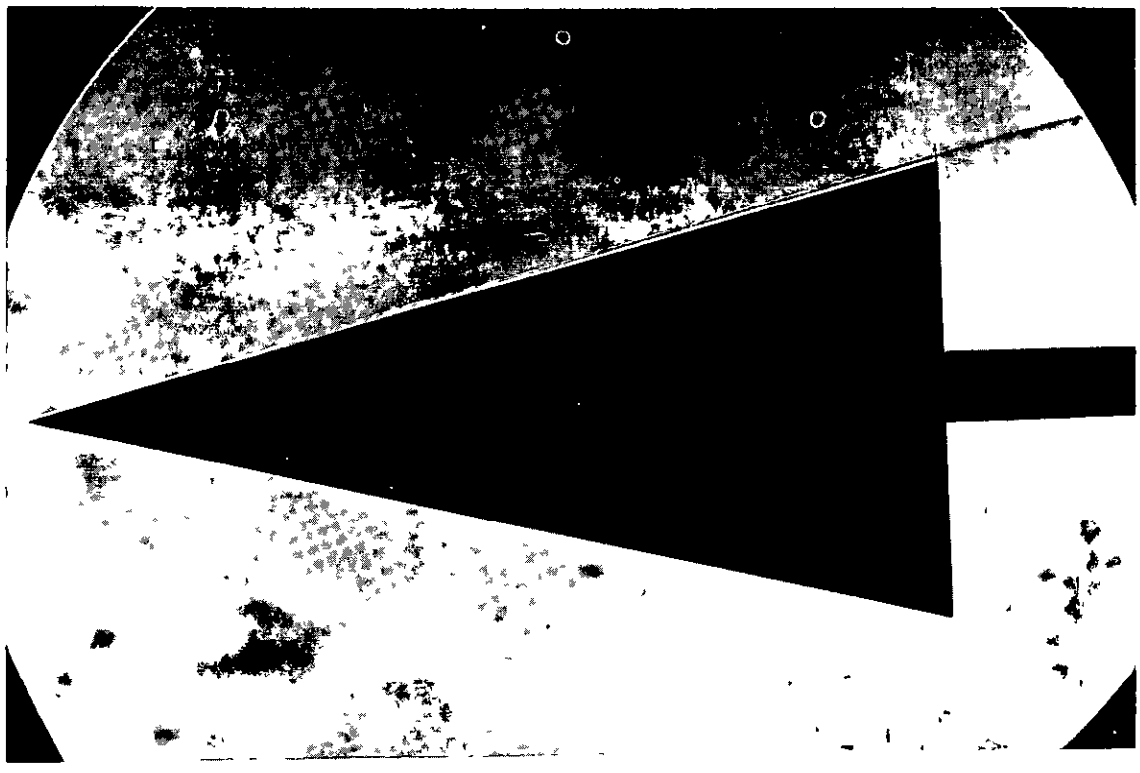

(e) Plain delta, $\alpha = 10^0$, $M = 8{\cdot}3$

Schlieren of flow (Plan view)

FIG. 12 (f & g)

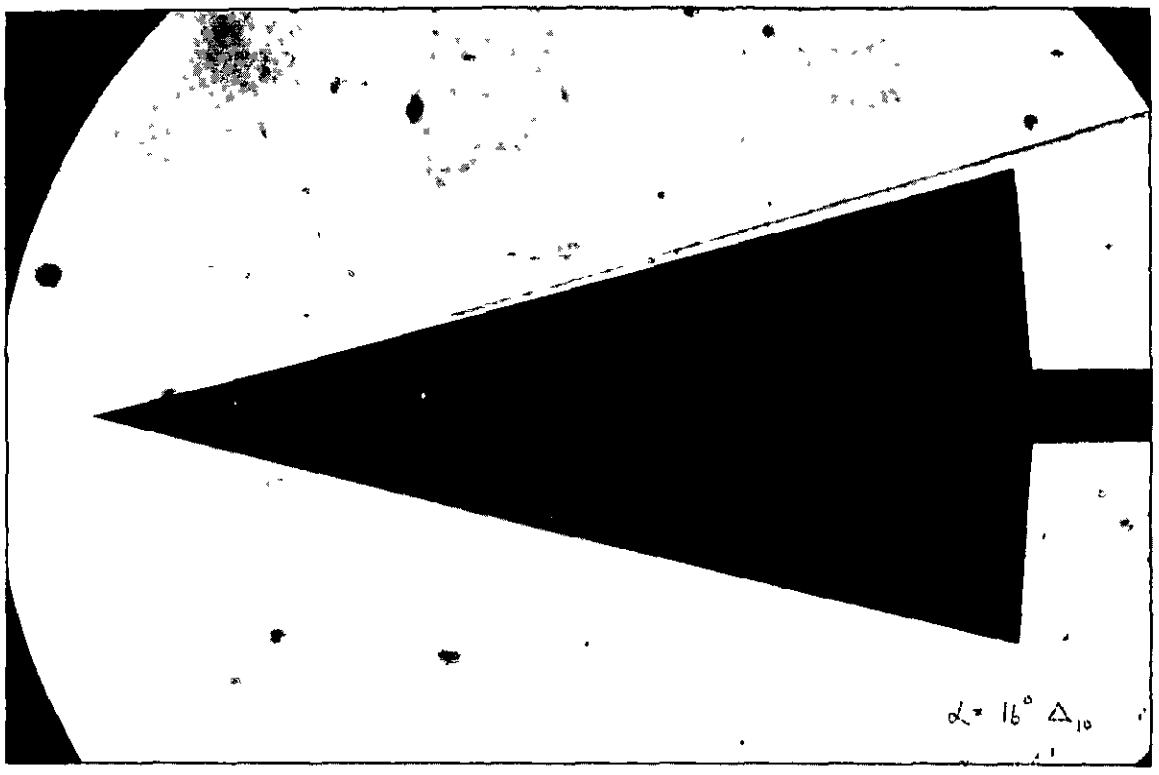

(f) Plain delta, $\alpha = 16^0$, M = 8·3

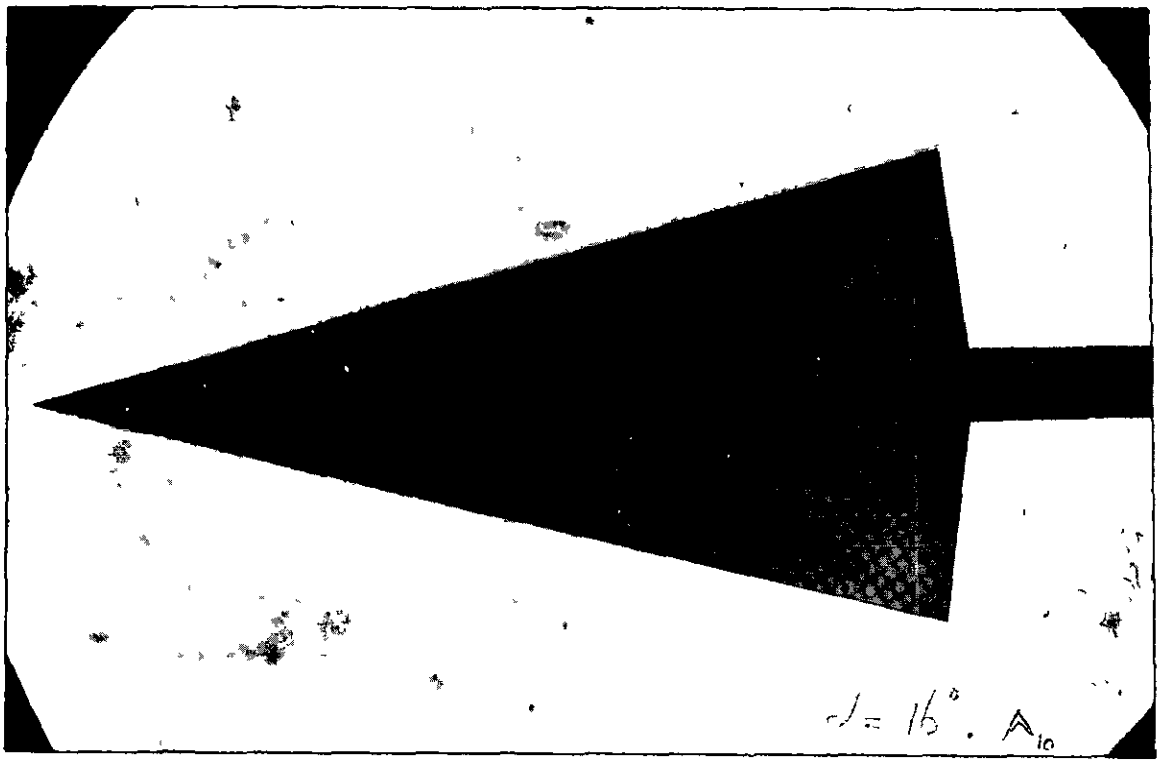

(g) Caret delta, $\alpha = 16^0$, M = 8·3

Schlieren of flow (Plan view)

FIG A1

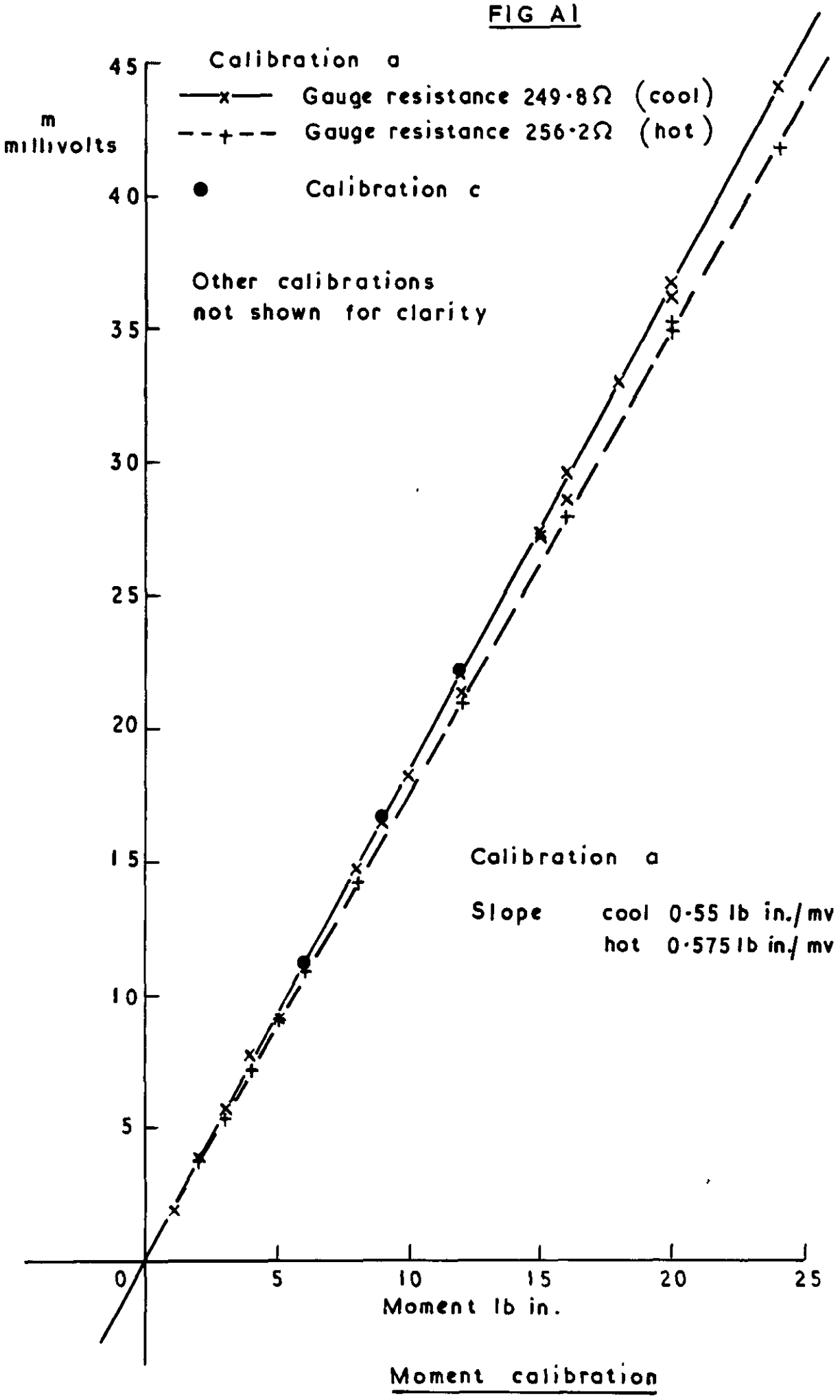

Moment calibration

FIG.A2

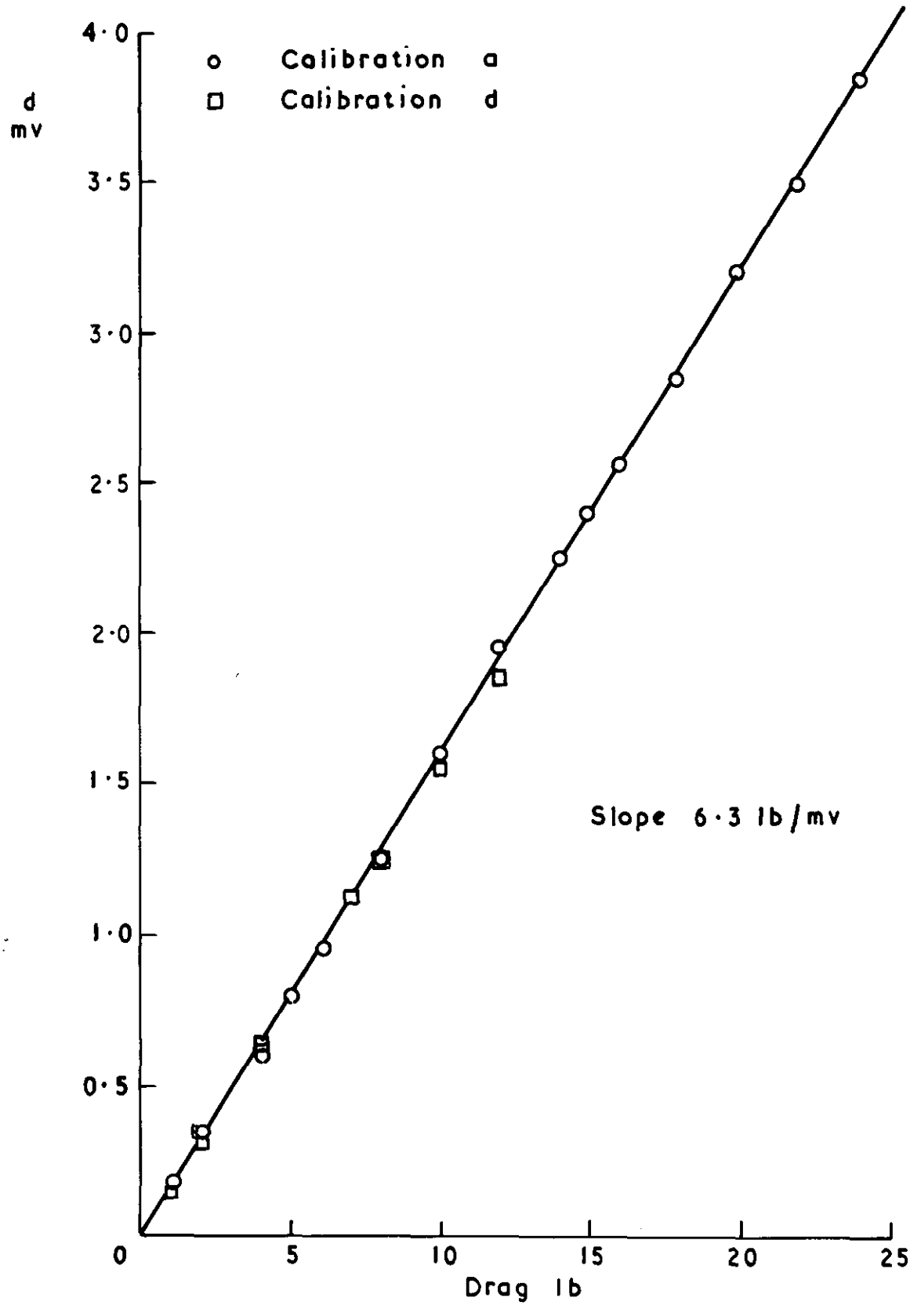

Drag calibration

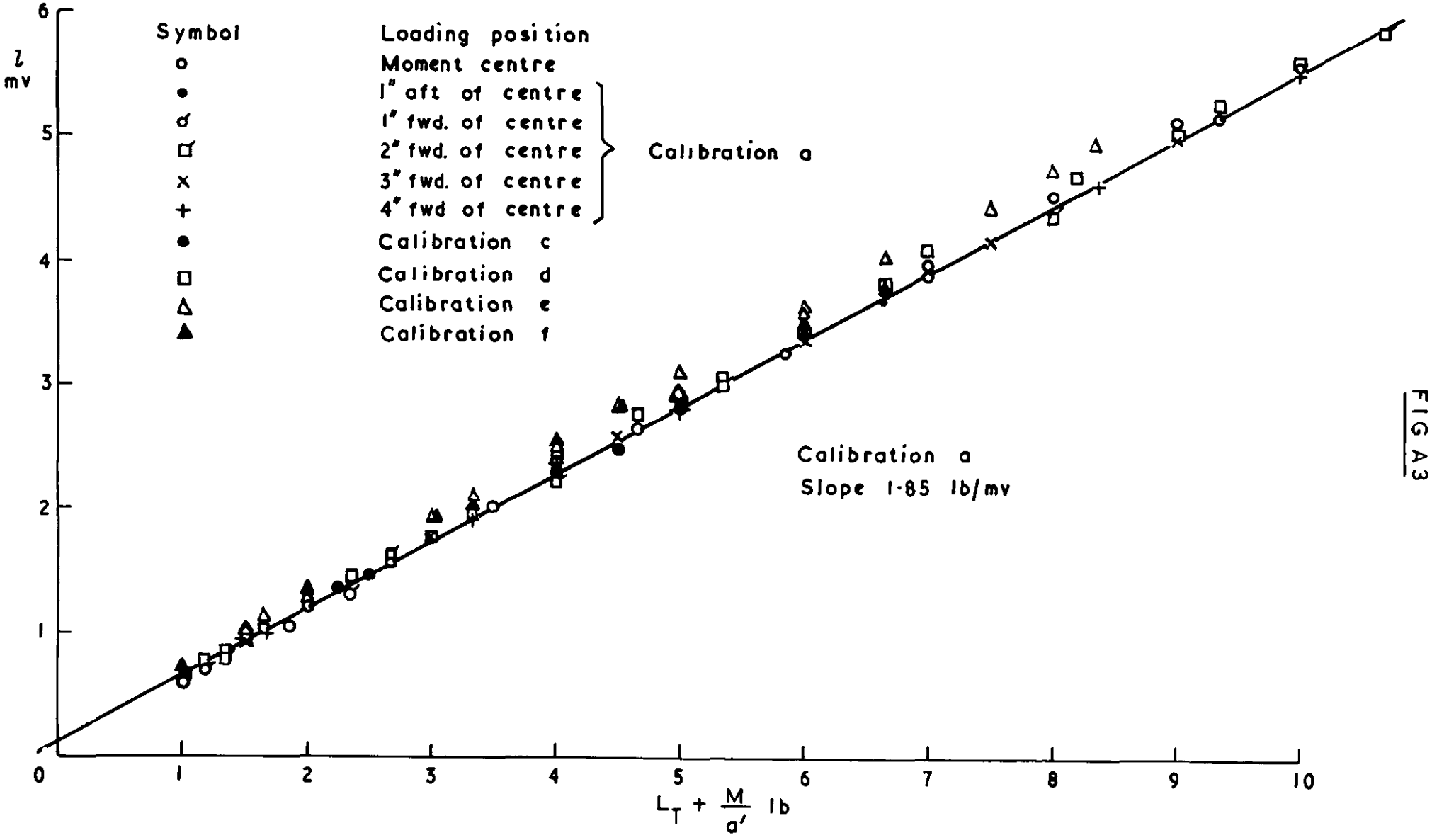

FIG A3

Lift calibration L_1 cantilever (fwd. lift sensor)

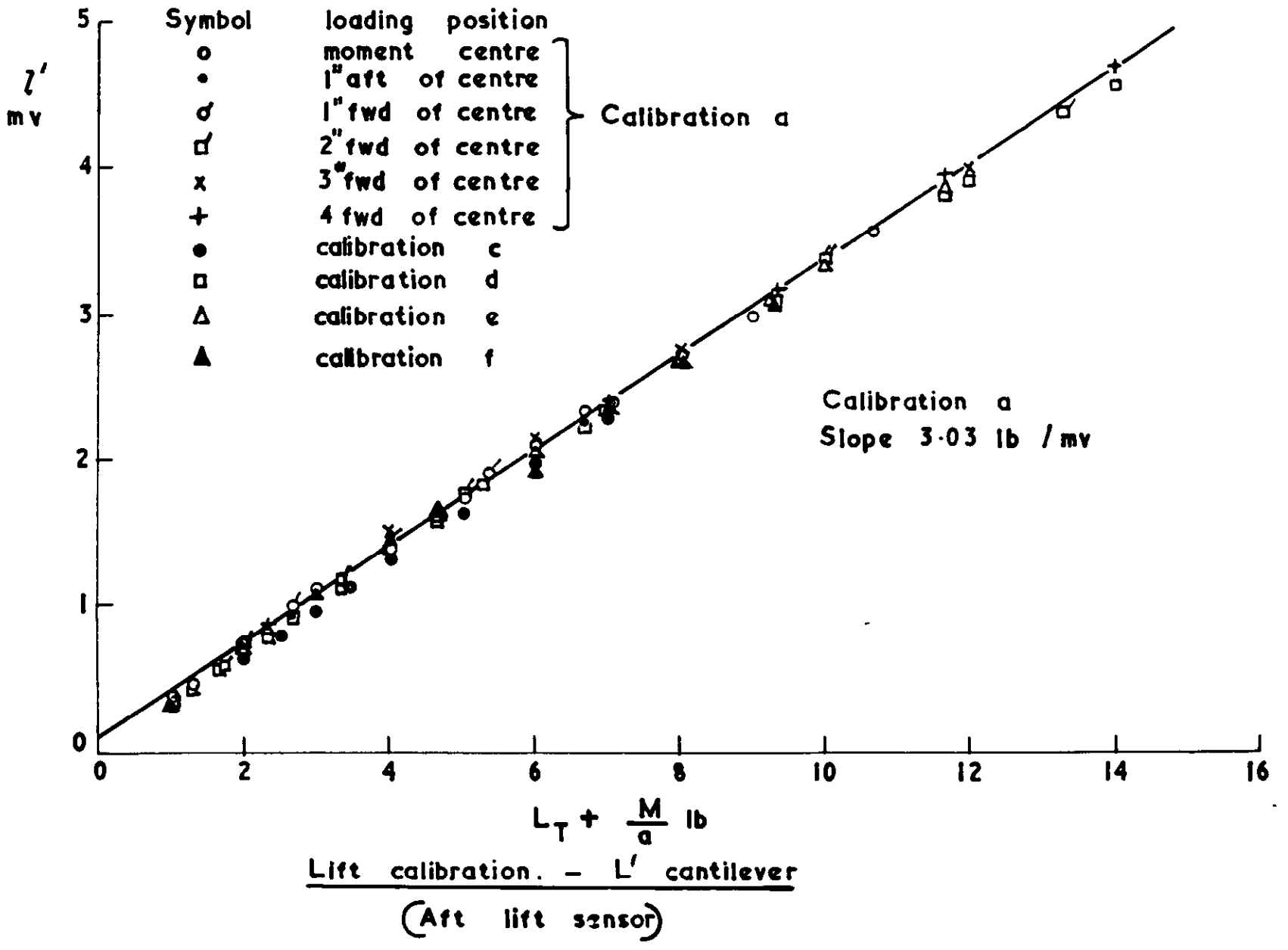
Symbol
loading position
o moment centre
• 1" aft of centre
1" fwd of centre
2" fwd of centre
x 3" fwd of centre
+ 4 fwd of centre
Calibration a
● calibration c
□ calibration d
Δ calibration e
▲ calibration f
l'
mv
Calibration a
Slope 3·03 lb / mv
0
1
2
3
4
5
0
2
4
6
8
10
12
14
16
$L_T + \frac{M}{a}$ lb
Lift calibration. – L' cantilever
(Aft lift sensor)

FIG. A 4

FIG. A 5

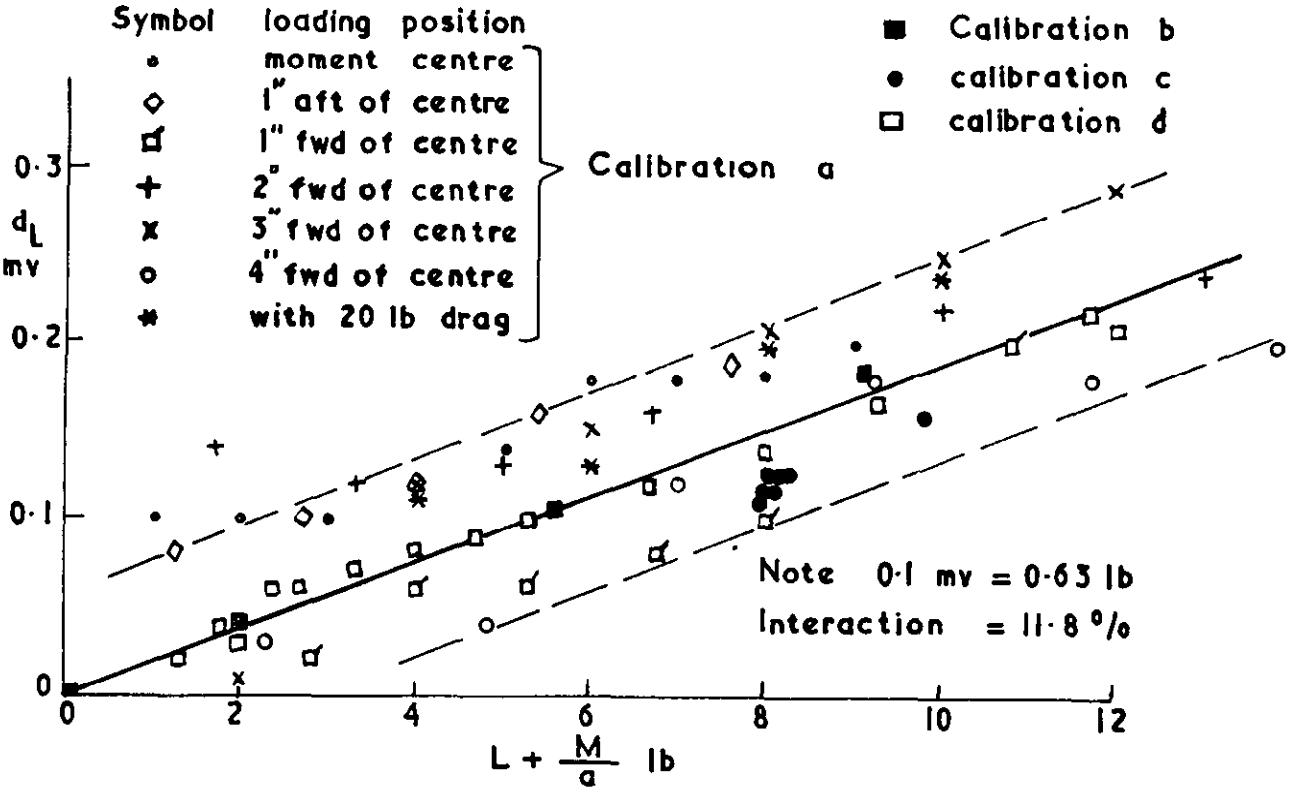

(a) Lift interaction on drag

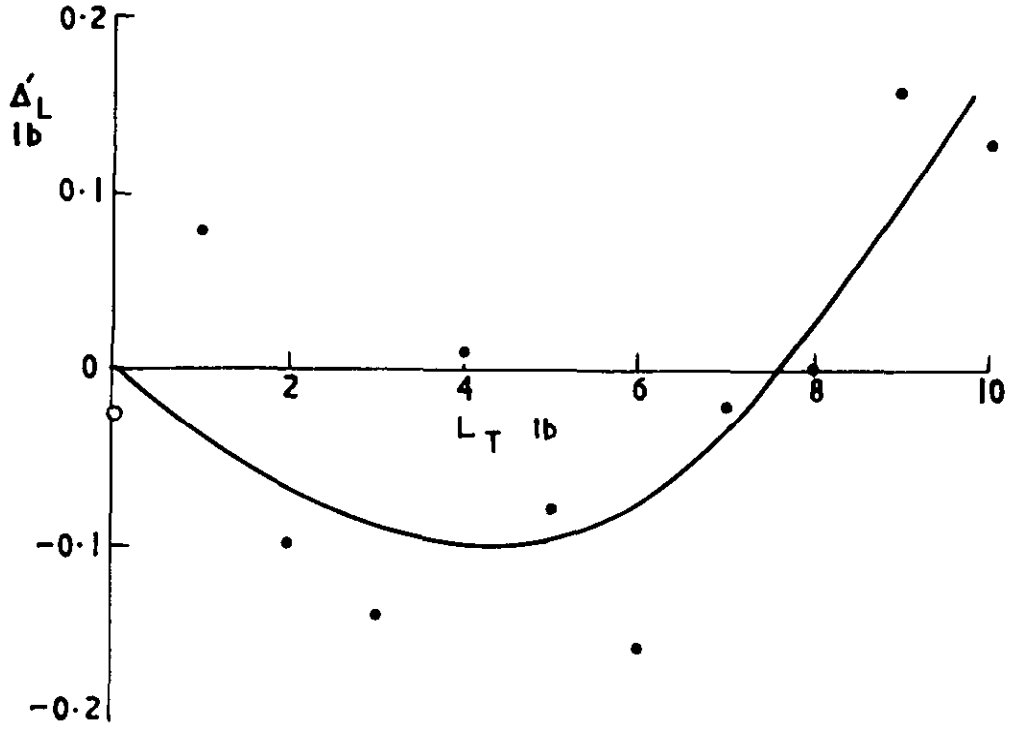

(b) Lift correction Δ'_L at zero moment.

See para. V

A.R.C. C.P. No.908
December, 1965
Opatowski, T. Imperial College of Science and Technology

GUN TUNNEL MEASUREMENTS OF LIFT, DRAG AND PITCHING MOMENT ON A 20° CONE, A FLAT DELTA AND A CARET DELTA WING AT A MACH NUMBER OF 8·3

Measurements of lift, drag and pitching moment have been made on a 20° half-angle, right-circular cone and on two delta wings of triangular and caret cross section, 10° wedge angle and aspect ratio 1 in the Imperial College gun tunnel.

The strain gauge balance developed for this purpose gave results which were within 5% of other published cone data.

Maximum lift/drag ratios of about 3·7 were obtained for both wings at the test Mach number of 8·3 and Reynolds number based on root chord of $1·5 \times 10^6$.

The measured lift, drag and lift/drag ratio agreed well with estimates based on two-dimensional oblique shock theory and laminar skin friction.

A.R.C. C.P. No.908
December, 1965
Opatowski, T. Imperial College of Science and Technology

GUN TUNNEL MEASUREMENTS OF LIFT, DRAG AND PITCHING MOMENT ON A 20° CONE, A FLAT DELTA AND A CARET DELTA WING AT A MACH NUMBER OF 8·3

Measurements of lift, drag and pitching moment have been made on a 20° half-angle, right-circular cone and on two delta wings of triangular and caret cross section, 10° wedge angle and aspect ratio 1 in the Imperial College gun tunnel.

The strain gauge balance developed for this purpose gave results which were within 5% of other published cone data.

Maximum lift/drag ratios of about 3·7 were obtained for both wings at the test Mach number of 8·3 and Reynolds number based on root chord of $1·5 \times 10^6$.

The measured lift, drag and lift/drag ratio agreed well with estimates based on two-dimensional oblique shock theory and laminar skin friction.

A.R.C. C.P. No.908
December, 1965
Opatowski, T. Imperial College of Science and Technology

GUN TUNNEL MEASUREMENTS OF LIFT, DRAG AND PITCHING MOMENT ON A 20° CONE, A FLAT DELTA AND A CARET DELTA WING AT A MACH NUMBER OF 8·3

Measurements of lift, drag and pitching moment have been made on a 20° half-angle, right-circular cone and on two delta wings of triangular and caret cross section, 10° wedge angle and aspect ratio 1 in the Imperial College gun tunnel.

The strain gauge balance developed for this purpose gave results which were within 5% of other published cone data.

Maximum lift/drag ratios of about 3·7 were obtained for both wings at the test Mach number of 8·3 and Reynolds number based on root chord of $1·5 \times 10^6$.

The measured lift, drag and lift/drag ratio agreed well with estimates based on two-dimensional oblique shock theory and laminar skin friction.

Printed and published by
HER MAJESTY'S STATIONERY OFFICE
To be purchased from
49 High Holborn, London W C 1
423 Oxford Street, London W.1
13A Castle Street, Edinburgh 2
109 St Mary Street, Cardiff
Brazennose Street, Manchester 2
50 Fairfax Street, Bristol 1
35 Smallbrook, Ringway, Birmingham 5
80 Chichester Street, Belfast 1
or through any bookseller

Printed in England

S.O. Code No 23-9017-8